# Serotonergic modulation of walking in *Drosophila*

Clare E. Howard [1,2], Chin-Lin Chen [3,4], Tanya Tabachnik [5], Rick Hormigo [5], Pavan Ramdya [3,4], Richard S. Mann [1]

1 Mortimer B. Zuckerman Mind Brain Behavior Institute, Columbia University, New York, NY, USA

2 Medical Scientist Training Program, Columbia University, New York, NY, USA

3 Brain Mind Institute, École Polytechnique Fédérale de Lausanne, CH-1015 Lausanne, Switzerland

4 Interfaculty Institute of Bioengineering, École Polytechnique Fédérale de Lausanne, CH-1015 Lausanne, Switzerland.

5 Advanced Instrumentation Group, Zuckerman Mind Brain Behavior Institute, Columbia University, New York, NY, USA

**Abstract**

To navigate complex environments, animals must generate highly robust, yet flexible, locomotor behaviors. For example, walking speed must be tailored to the needs of a particular environment: Not only must animals choose the correct speed and gait, they must also rapidly adapt to changing conditions, and respond to sudden and surprising new stimuli. Neuromodulators, particularly the small biogenic amine neurotransmitters, allow motor circuits to rapidly alter their output by changing their functional connectivity. Here we show that the serotonergic system in the vinegar fly, *Drosophila melanogaster*, can modulate walking speed in a variety of contexts and in response to sudden changes in the environment. These multifaceted roles of serotonin in locomotion are differentially mediated by a family of serotonergic receptors with distinct activities and expression patterns.

## Introduction

Insects have a remarkable capacity to adapt their locomotor behaviors across a wide range of environmental contexts and to confront numerous challenges. For example, they can walk forwards, backwards, and upside down, navigate complex terrains, and rapidly recover after injury [1-9]. To achieve this wide range of behaviors, insects regulate their global walking speed and kinematic parameters, allowing them to modify stereotyped gaits as needed [3,5-7,9,10]. Because overlapping sets of motor neurons and muscles are recruited for all of these behaviors, animals must be able to rapidly modulate the circuit dynamics that control locomotor parameters [11-13] (reviewed in [14]).

As with limbed vertebrates, most insects use multi-jointed legs to walk [8,10,15-17]. Locomotor circuits that orchestrate these complex gaits are located in the ventral nerve cord (VNC), a functional analogue of the vertebrate spinal cord that includes three pairs of thoracic neuromeres (T1, T2, and T3) that coordinate the movements of the three pairs of thoracic legs [1-9,18-20]. The insect VNC receives descending commands from the brain and sends motor output instructions via motor neurons to peripheral musculature [3,5-7,9,10,19]. Leg motor neuron dendrites innervate the leg neuropils within the VNC and their axons exit the VNC to synapse onto muscles in the appendages [11-13,21,22]. Sensory neurons, which convey proprioceptive and tactile information, project axons from the appendages to the VNC by these same fiber tracts, where they arborize in the leg neuropils [14,23,24] (Figure 1A). Notably, the VNC is capable of executing coordinated leg motor behaviors, such as walking and grooming, even in decapitated animals [8,10,15-17,25]. Thus, the VNC harbors neural networks that can drive the coordinated flexion and extension of each leg joint and, therefore, walking gaits [8,10,17,20,26].

Numerous studies have shown that sensory input from the legs are required for robust and stereotyped locomotor patterns, regulating both the timing and magnitude of locomotor activity and also facilitating coordination between legs [6,8,10,12,27-29]. However, sensory feedback cannot be the only means for tuning locomotion: mutation of proprioceptive receptors or even deafferenting limbs does not block coordinated walking [10,15,18,30-33]. Beyond sensory feedback-driven tuning of gait patterns, larger behavioral changes must be accomplished by other circuits. These likely include neuromodulatory systems, including the monoamines dopamine, norepinephrine, and serotonin, which are highly conserved throughout the animal kingdom.

Monoamines have been shown to modulate, and even induce, the activities of central pattern generating (CPG) motor circuits. In crustaceans, for example, neuromodulation causes the gastric CPG to generate distinct rhythmic activity patterns from the same neural network to address distinct behavioral demands [34-39] (reviewed in [13,40]). Remarkably, the same neuromodulatory systems appear to play similar roles across species. For example, serotonin has been shown to slow locomotor rhythms in animals as diverse as the lamprey, cat, and locust [41-43]. In the vinegar fly, *Drosophila melanogaster,* monoamine neurotransmitters have also been shown to modulate walking behavior. In addition to slowing walking speed, serotonin modulates sleep and anxiety-related motor behaviors [3,5,6,9,10,44-48]. Dopamine, in contrast, has been linked to hyperactivity [25,49-52]. Octopamine has been shown to mediate starvation induced hyperactivity, and in its absence animals walk more slowly [8,53,54]. As each of these neuromodulatory systems plays a variety of roles in regulating complex behaviors, it has thus far been challenging to tease apart which of the effects on walking behavior are due to direct modulation of motor circuitry or are a secondary consequence of modulating higher order circuits in the brain.

In this work, we show that the serotonergic neurons within the VNC can modulate walking speed in a context-independent manner as well as in response to startling stimuli. Additionally, we demonstrate that these modulatory effects are enacted through serotonin's action via specific receptors that are expressed in different parts of the locomotor circuit. Together, these findings reveal that neuromodulatory systems regulate multiple aspects of complex behaviors such as walking at multiple time scales, allowing animals to effectively respond to rapidly changing environments.

## Results

### VNC serotonergic neurons arborize within the leg neuropils

To identify neuromodulatory neurons that might play a role in modulating walking behavior we drove expression of a fluorescent reporter with Gal4 under the control of promoters encoding key synthetic enzymes for each neuromodulatory system – *Tryptophan hydroxylase* (*Trh* for serotonin (5-HT) [55]); *tyrosine hydroxylase* (*TH* or *ple* (*pale*) for dopamine [56]); and *Tyrosine decarboxylase 2* (*Tdc2* for octopamine and tyramine [57]). All of these drivers show extensive expression in cells both within the VNC and the brain, with processes that densely innervate VNC leg neuromeres (Figure 1) [55].

To determine whether local VNC neurons or descending neurons originating in the brain innervate the leg neuropils, we used genetic intersectional tools to limit the expression of these Gal4 lines to either the brain or VNC (Figure 1A). These experiments show that neuromodulatory innervation of the leg neuropils arises almost entirely from VNC interneurons and not from descending neurons in the brain (Figure 1B-G). Moreover, in many cases, these VNC neurons extensively innervate the leg neuropils. Thus, VNC neuromodulatory neurons are well-positioned to directly modulate VNC locomotor circuits. These intersectional genetic tools therefore allow us to assess the behavioral role of local VNC neuromodulation independently of modulation within higher brain regions.

Figure 1

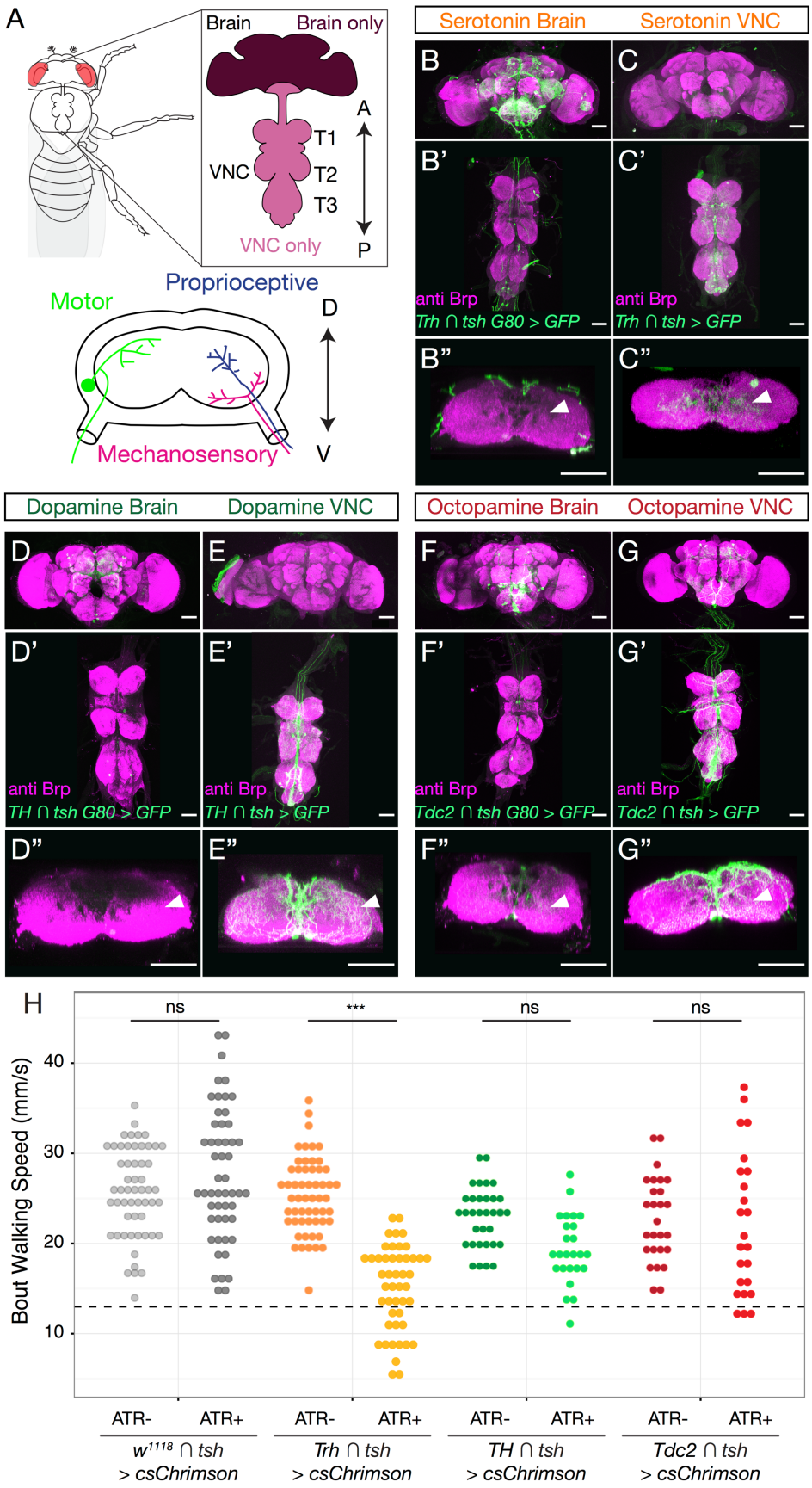


102

**Figure 1. Neuromodulators in the fly CNS.**

**A.** The adult *Drosophila* CNS is composed of the brain and the VNC, which consists of three thoracic neuropils (T1, T2 and T3), each of which corresponds to a pair of adult legs, and an abdominal ganglion. Anterior-posterior axis specified. *Lower panel:* Each thoracic neuropil contains the projections of locomotor circuit components, including motor neurons that send axons to leg muscles and sensory neurons that convey mechanosensory and proprioceptive information from the legs (schematized here in cross section). Dorsal – ventral axis specified.

**B-G.** Maximum intensity projections show the expression patterns driven by Gal4 lines labeling either brain-derived (B, D, F, *Gal4* intersected with *tsh Gal80*) or VNC-derived (C, E, G, *Gal4* intersected with *tsh*) serotonergic (B-C, *Trh Gal4*), dopaminergic (D-E, *TH Gal4*), or octopaminergic/tyraminergic (F-G, *Tdc2 Gal4*) neurons. (B''-G'') Projection of a subset of cross sections of the VNC shows innervation of the T1 neuropil. All scale bars are 50 um.

**H.** Optogenetic activation of serotonergic (*Trh-Gal4*) neurons in the *Drosophila* VNC, but not dopaminergic (*TH-Gal4*) or octopaminergic/tyraminergic (*Tdc2-Gal4*) neurons, slows walking speed compared to all-trans-retinal (ATR) negative and non-Gal4 ($w^{1118}$) controls. These activation experiments were carried out using the Flywalker assay (Mendes et al., 2013; see Figure S3A for a schematic). Statistics computed using a Kruskal-Wallis test with the Dunn-Sidak correction for multiple comparisons * <.05 **<.01 ***<.001. N walking bouts (animals) $w^{1118}$ ATR- 55 (14-31); $w^{1118}$ ATR+ 52 (14-36); *Trh* ATR- 56 (12-30); *Trh* ATR+ 47 (10-23); *TH* ATR- 33 (10-24); *TH* ATR+ 25 (10-26); *Tdc2* ATR- 27 (10-27); *Tdc2* ATR+ 24 (10-25).

**Activation of VNC serotonergic neurons slows walking speed**

Previous studies showed that neuromodulatory systems can regulate walking [8,25,47,49,51,54,58], but could not dissociate the relative contribution of brain and VNC neuromodulatory subpopulations. Here we addressed whether neuromodulatory neurons in the VNC alone are sufficient to modulate walking behavior. We specifically optogenetically activated these neurons and found that activation of serotonergic VNC populations, but not dopaminergic or octopaminergic/tyraminergic VNC subpopulations, altered the average speed at which animals walk (Figure 1H).

Based on these results, we focused the remainder of our analysis on VNC serotonergic neurons (5-HT$^{VNC}$). To validate the fidelity of our serotonergic Gal4 driver line, and to rule out co-secretion of other neurotransmitters, we performed immunostaining for markers of serotoninergic (5-HT), dopaminergic (TH), octopaminergic/tyraminergic (Tdc2), glutamatergic (VGlut), cholinergic (ChAT), and GABAergic (GABA) neurons (Figure S1). These experiments demonstrate that the *Trh-Gal4* line drives expression in 5-HT-expressing neurons, and that these neurons do not express any of the other neurotransmitters we surveyed, suggesting that they are primarily serotonergic.

We next confirmed the effects of activating 5-HT$^{VNC}$ neurons by studying animals freely walking within an arena. This allowed us to measure not only an animal's speed, but also its walking frequency, angular velocity, and preferred position within the arena (Figure S2A-C). As with our initial experiments, activation of 5-HT$^{VNC}$ neurons is sufficient to produce a rapid slowing of average walking speed in this paradigm (Figure 2A). Interestingly, activation of 5-HT$^{VNC}$ neurons does not change the overall amount of time animals spend walking, suggesting that speed changes are not simply due to a decrease in overall activity, but instead reveal a bias towards slower walking speeds (Figure S2D and F). Unlike a previous study showing that overexpressing the serotonin transporter in all neurons caused flies to move away from the edge of the arena [46], we see no effect on the distribution of animals within the arena when we limit the activation to 5-HT$^{VNC}$ neurons (Figure S2D). We also find that activation of 5-HT$^{VNC}$ neurons decreases the absolute angular velocity of walking flies (Figure S2D). Thus, although these flies walk slower, they also walk straighter than control flies. This latter observation is unexpected, because straighter trajectories are usually correlated with faster walking speeds (Figure S2F) [10].

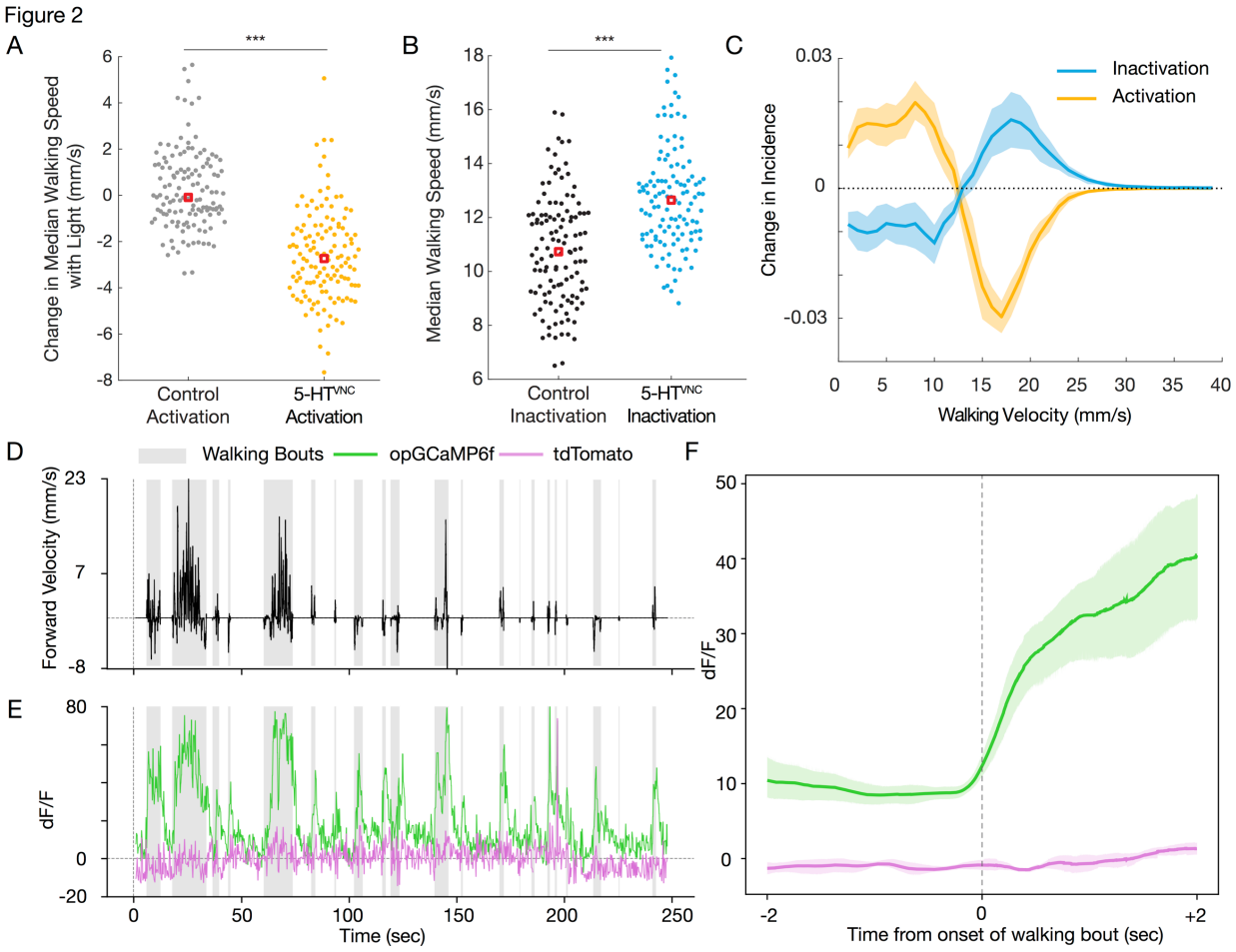


**Figure 2. 5-HT$^{VNC}$ neurons modulate walking speed.**

**A.** Activation of 5-HT$^{VNC}$ neurons (*Trh ∩ tsh > csChrimson* fed with ATR) causes animals to walk slower than background matched non-Gal4 controls ($w^{1118}$ *∩ tsh >csChrimson* fed with ATR). Both genotypes were fed all-trans-retinal. Genotypes were compared using Kruskal-Wallis test, ***p<.001. N = 130 animals for each condition.

**B.** Inactivation of 5-HT$^{VNC}$ neurons (*Trh ∩ tsh > Kir2.1*) causes animals to walk faster than genetically matched non-Gal4 controls ($w^{1118}$ *∩ tsh > Kir2.1*). Genotypes were compared using a Kruskal-Wallis test, ***p<.001. N=119 animals per genotype.

**C.** The distribution of velocity shifts caused by activation and inhibition of 5-HT$^{VNC}$ neurons are symmetrical. Differences in population average histograms were calculated between control and experimental genotypes and were fit with 95% confidence intervals via bootstrapping. For activation experiments, behavior of $w^{1118}$ *∩ tsh >csChrimson* flies fed with ATR was compared to that of *Trh ∩ tsh >csChrimson* flies also fed with ATR for the light on period only.

**D, E.** Serotonergic processes passing through the cervical connective (labeled using *Trh ∩ tsh*) are active during walking. **(D)** A single animal's forward velocity with overlaid boxes showing defined walking bouts. **(E)** While tdTomato baseline signal (purple line) is not affected by walking bouts, the calcium signal (green line) in these serotonergic processes rises during walking bouts (gray boxes).

**F.** Fluorescent signal in these processes rises with the onset of walking bouts. For each animal, all walking bouts were synchronized around their onset, and an average was taken (between 80 and 130 walking bouts per animal). Plotted is the average of all animals (N=5) with a 95% confidence interval representing the spread between animals.

## Flies with activated 5-HT$^{VNC}$ neurons walk in a coordinated manner

Slower walking speeds could be the result of poor coordination or, alternatively, controlled adjustments of gaits, which occur when flies walk upside down or carry an additional load [7]. To distinguish between these two possibilities, we analyzed fly gaits using the Flywalker assay [10]. This system uses frustrated total internal reflection to visualize an animal's footprints during a walking bout and custom software to analyze these footprints, generating an array of kinematic measurements (Figure S3A) [10].

Using this assay, we find that activation of 5-HT$^{VNC}$ neurons results in highly coordinated walking patterns. Representative traces of an individual's footprints during a walking bout show that activation of these neurons does not perturb stereotyped foot placement or interfere with the straightness of the stance phase (Figure 3A and C). Step and stance traces show that these animals also use highly coordinated gaits, suggesting that interleg coordination is intact (Figure 3B and D). In fact, compared to control flies, 5-HT$^{VNC}$ neuron activation results in more precise foot placement at the onset and offset of each stance phase, suggesting that the walking behavior of these animals is more constrained compared to control animals (Figure S3B).

In wild type flies, most locomotor parameters are highly correlated with speed, shifting as animals walk faster or slower. Activation of 5-HT$^{VNC}$ neurons induces kinematic shifts that extrapolate these relationships to speeds not normally accessed by wild type flies. For example, as animals walk slower, their step cycle frequency decreases, they take longer steps, and slow the velocity of their swinging legs. These shifts are accompanied by a shift in the step duty cycle, as stance duration increases while swing duration remains largely unchanged [10]. These relationships are maintained and extended into the slower speed range when 5-HT$^{VNC}$ neurons are activated (Figure 3E-I).

In contrast to the kinematic parameters described above, the relationship between gait and speed is not a simple extrapolation upon 5-HT$^{VNC}$ neuron activation. For example, as animals walk more slowly, their preferred gait shifts from the three-legged tripod gait to the more stable tetrapod and wave gaits [8,10]. Upon activation of 5-HT$^{VNC}$ neurons, the slope of a subset of these relationships (tripod and wave gait in particular) shifts (Figure 3J and L). Thus, in

addition to maintaining the relationships between speed and most kinematic parameters, serotonin alters the relationship between particular types of gait choice and walking speed.

Figure 3

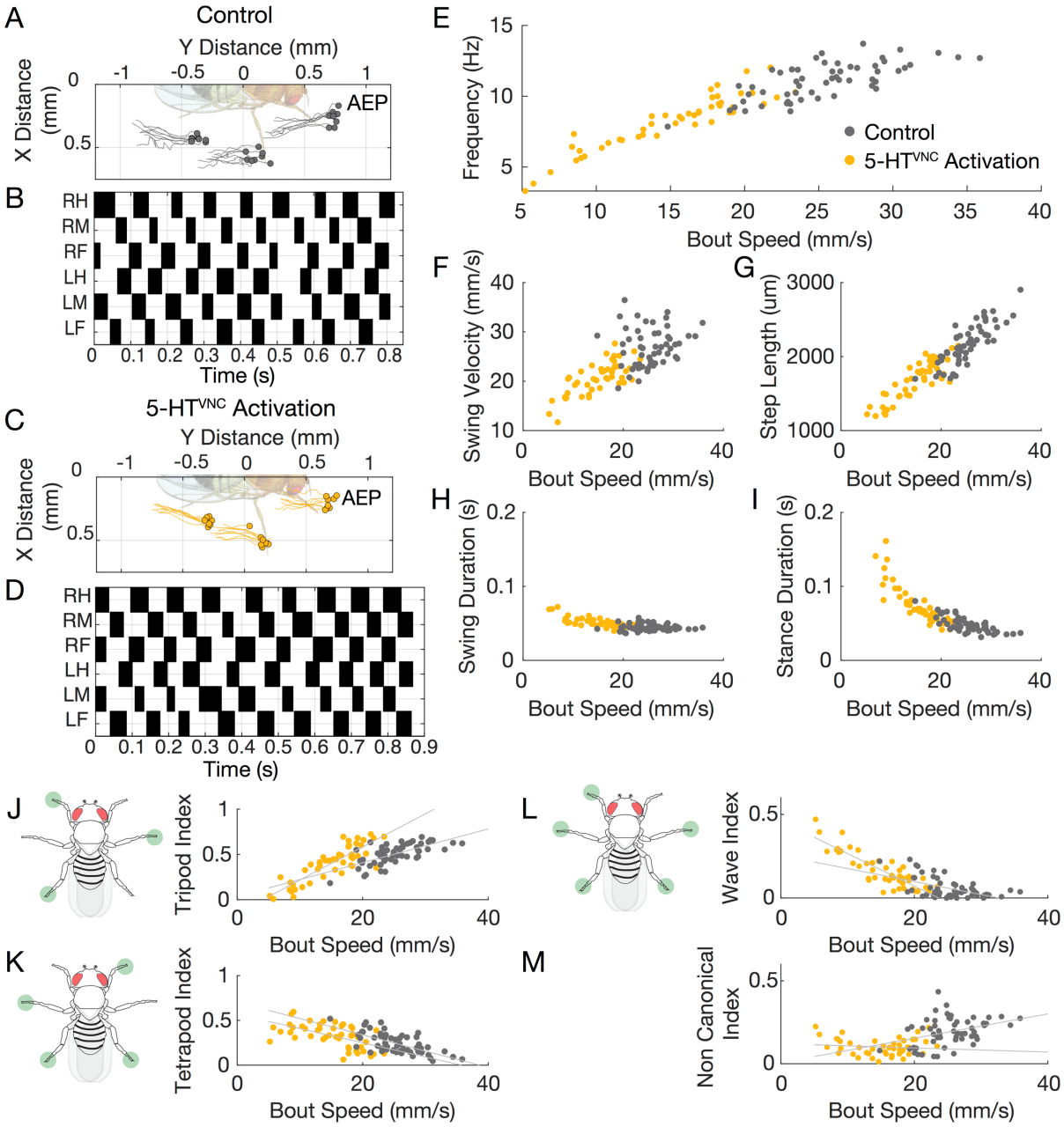


**Figure 3. Activation of 5-HT$^{VNC}$ neurons extrapolates most locomotor kinematics.**

**A-D.** Representative data from speed-matched slow (19 mm/s) walking bouts show that activation of 5-HT$^{VNC}$ neurons does not disrupt locomotor coordination. Footfalls (filled circles) and stance traces (lines) for all steps taken by the left front, middle, and hind legs show foot touchdown placement is consistent over time and stance traces are relatively straight in both control animals (*Trh* ∩ *tsh* >*csChrimson* grown on food lacking ATR) (A) and animals where 5-HT$^{VNC}$ neurons have been activated (*Trh* ∩ *tsh* >*csChrimson* fed with ATR) (C). Step trace for each leg during a walking bout for control (B) and experimental (D) animals. Stance phase is

indicated in white and swing phase in black. The checkerboard pattern is consistent with a highly-coordinated walking gait.

**E-I.** Extrapolation of step parameters upon activation of 5-HT$^{VNC}$ neurons. The relationships between speed and frequency (E), swing velocity (F), step length (G), swing duration (H), and stance duration (I) are shifted in a manner that is consistent with normal walking speeds. N = 47 bouts from 10-23 animals for *Trh* ∩ *tsh* >*csChrimson* ATR+ (yellow circles). N=56 bouts from 12-30 animals for *Trh* ∩ *tsh* >*csChrimson* ATR- (gray circles).

**J-M.** Activation of 5-HT$^{VNC}$ neurons modifies the relationship between speed and gait selection. Activation of 5-HT$^{VNC}$ neurons increases wave (L) and tetrapod (K) gait utilization while decreasing time spent using tripod (J) gait. There is a low frequency of non-canonical gait conformations upon activation (M). p<.001 for speed by ATR interaction effect in multivariable model for tripod index and wave index. N = 47 bouts from 10-23 animals for *Trh* ∩ *tsh* >*csChrimson* ATR+ (yellow circles). N=56 bouts from 12-30 animals for *Trh* ∩ *tsh* >*csChrimson* ATR- (gray circles).

## Inhibition of 5-HT$^{VNC}$ neurons increases walking speed

Although the experiments described above demonstrate that activation of 5-HT$^{VNC}$ neurons causes flies to walk more slowly, gain-of-function experiments such as these cannot address if and in what situations these neurons are normally used to modulate walking speed. To begin to address this question, we expressed the inward rectifying potassium channel Kir2.1 to constitutively inactivate 5-HT$^{VNC}$ neurons [59]. Although neurons were inactivated throughout development and adulthood, we did not observe a change in the number or anatomy of these neurons in the VNC, suggesting that their development is not significantly affected (Figure S2H and I).

Consistent with the activation phenotype, inhibition of 5-HT$^{VNC}$ neurons causes animals to walk faster (Figure 2B) and increases their angular velocity (Figure S2E and G). Inhibiting these neurons also increases the percentage of time that animals spend walking (Figure S2E).

The shifts in velocity produced by either optogenetic activation or constitutive inhibition of 5-HT$^{VNC}$ neurons mirror each other (Figure 2C). In both cases, ~12 mm/s is the boundary between velocities that are lost and gained due to 5-HT$^{VNC}$ neuron manipulation (Figure 2C). These complementary shifts in walking speed suggest that serotonin release in the VNC may serve as a switch to regulate behavioral state.

## 5-HT$^{VNC}$ neurons are active in walking flies

The opposing effects on speed when 5-HT$^{VNC}$ neurons are activated or inhibited suggest that the activity of these neurons will co-vary with walk-stop transitions and velocity changes

during baseline walking. To test this prediction, we performed functional calcium imaging of a subset of 5-HT$^{VNC}$ axons within the VNC while flies walked on a spherical treadmill (Figure S4A) [60]. To record the largest functional signals, we focused on axons in the neck connective, which are likely derived from the subset of ascending 5-HT$^{VNC}$ neurons that target the brain (Figure S4B-D).

Activity in these fibers is highly correlated with walking (Figure 2D and E). Fluorescence signals from these cells rise dramatically at the onset of each walking bout (Figure 2F). These responses are not nearly as large when animals perform other motor behaviors, like proboscis extension or grooming (Figure S4E). These results suggest that at least a subset of 5-HT$^{VNC}$ neurons are specifically active when flies walk, and are not generically active during all legged motor behaviors. We also find that the activity of these serotonergic processes correlates with the average speed of the walking bout, suggesting that these neurons may become more active when animals walk faster (Figure S4F). These observations are particularly interesting in the context of our other behavioral data, which show that walking speed can be shifted faster or slower by manipulating 5-HT$^{VNC}$ neural activity. Thus, baseline walking speed correlates with but is also sensitive to 5-HT$^{VNC}$ neural activity. Taken together, these observations suggest that one role for serotonin release in the VNC may be to dampen walking speed, a conclusion that we further test below.

**Serotonin slows baseline walking in multiple contexts**

Results from optogenetic activation and recordings can be reconciled by a model whereby the VNC serotonergic system is used to regulate walking speed: when the system is activated, flies walk more slowly and when the system is silenced, flies walk faster. To test this model, we asked if 5-HT$^{VNC}$ neural activity is required when flies naturally alter their walking speeds. For example, flies normally walk at different speeds depending on ambient temperature, body orientation, nutritional status, and in response to mechanosensory stimulation [2,7,61,62]. Surprisingly, animals in which 5-HT$^{VNC}$ neurons were silenced were still able to adjust their speed in the same direction as wild type flies in all of these contexts (Figure 4A). Moreover, regardless of the context, animals in which these neurons are silenced walk faster than controls. Thus, animals do not require 5-HT$^{VNC}$ neuron activity to modulate their speed in response to different environmental contexts (e.g. temperature), or internal state (e.g. hunger). Furthermore, these data suggest that this system is used in a context-independent manner to dampen walking speed.

298

299 **VNC serotonin release is required on a fast time scale to respond to rapid contextual**
300 **changes**

301 Another scenario in which animals may benefit from slowing down is when they are
302 startled. In mammals, stereotyped startle behaviors occur in response to a wide variety of
303 sensory stimuli – acoustic, tactile, and vestibular. These responses take place on sub-second
304 time scales, involve simultaneous contraction of muscles throughout the body, and are similar
305 irrespective of the initiating stimulus [63-65]. Like mammals, *Drosophila* display stereotyped
306 responses to threatening looming stimuli, beginning with an initial freezing period lasting less
307 than a second before escape behaviors are initiated [66,67]. Because these startle responses
308 are contextually independent and have been shown to be mediated in part by serotonin in
309 mammals [68], we next asked whether 5-HT$^{VNC}$ neurons are required for these responses in
310 *Drosophila.*

311 We tested this prediction using two different startle-inducing paradigms: (i) one in which
312 flies abruptly experience total darkness ('blackout paradigm') and (ii) one in which flies suddenly
313 experience strong mechanical stimulation, such as an intense vibration ('earthquake paradigm')
314 [62]. In both scenarios, control animals show a two-tiered response to these abrupt changes
315 (Figure 4B and C): First, animals rapidly come to a nearly complete stop. Then, they pause
316 before resuming a behavior that is appropriate for the new context. For both the blackout and
317 earthquake paradigms, control animals stop within the first 0.25 seconds, pause for about a
318 second, and only then resume walking behavior (Figure 4B and C, Figure S5B and D). Animals
319 lacking the ability to release serotonin in the VNC are deficient in these initial responses, but are
320 still able to eventually achieve context-appropriate walking speeds (Figure 4A). Moreover,
321 consistent with our earlier analyses, flies unable to activate 5-HT$^{VNC}$ neurons walk faster
322 compared to control flies, both before and after the change in their environment (Figure 4B and
323 C).

324 Taken together, these results demonstrate that the VNC serotonergic system is not
325 required for animals to modify their walking speed in response to changes in the environment or
326 shifts in internal state. In addition, they suggest that this system is needed for an immediate
327 and stimulus-independent response when flies are startled.

Figure 4

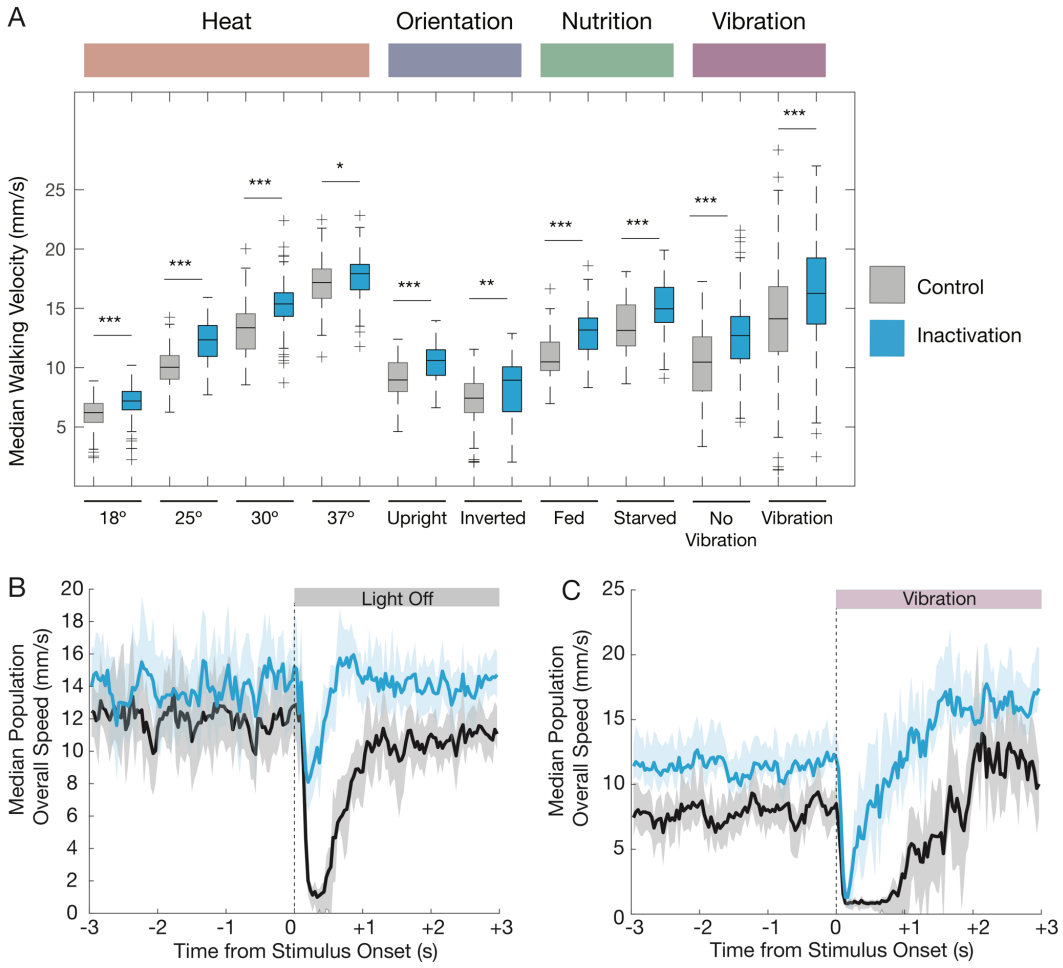


328

329 **Figure 4. Context-independent and context-specific roles of serotonin in locomotion.**

330 **A.** Silencing 5-HT$^{VNC}$ neurons (*Trh* ∩ *tsh* > *Kir2.*1) causes an increase in walking speed
331 compared to genetically background matched non-Gal4 controls ($w^{1118}$ ∩ *tsh* > *Kir2.1*) across a
332 diversity of behavioral contexts including variations of temperature, orientation, nutritional state,
333 and vibration stimuli. For each condition, genotypes were compared using a Kruskal-Wallis test,
334 ***p<.001, **p<.01, *p<.05. 18 °C– N=130 per genotype. 25 °C – N = 120 per genotype. 30 °C –
335 N = 120 per genotype. 37 °C – N= $w^{1118}$ (120) *Trh* (119). Upright – N = 90 per genotype.
336 Inverted – N=90 per genotype. Fed – N=86 per genotype. Starved – N = 86 per genotype.
337 Vibration – N= $w^{1118}$ (167) *Trh* (166).
338
339 **B-C.** Silencing 5-HT$^{VNC}$ neurons changes the immediate behavioral responses to sudden
340 contextual changes. When lights switch from on to off (B), control animals ($w^{1118}$ ∩ *tsh* > *Kir2.1*,
341 shown in black) show a brief behavioral pause (indicated by arrow) and then resume activity.
342 However, when 5-HT$^{VNC}$ neurons are silenced, animals slow their speed but do not fully pause.
343 In response to the onset of vibration (C) control animals stop, pause and then accelerate speed.
344 When 5-HT$^{VNC}$ neurons are silenced (*Trh* ∩ *tsh* > *Kir2.*1, shown in blue), animals pause but re-

accelerate more quickly than controls. Shaded areas show 95% confidence intervals. For light experiments, N= $w^{1118}$ (150) *Trh* (140); for vibration experiments N= $w^{1118}$ (167) *Trh* (166).

**Different serotonin receptor mutants alter the startle response in different ways**

All five serotonergic receptors in *Drosophila* – 5-HT1A, 5-HT1B, 5-HT2A, 5-HT2B, and 5-HT7 – are G-protein coupled receptors (GPCRs) [69-72]. Like their mammalian orthologs, members of each serotonin receptor family (1, 2, and 7) have distinct cellular effects upon activation. Receptors in the 1 family, 5-HT1A and 5-HT1B, act through the $G_i$ pathway to inhibit the generation of cAMP, whereas 5-HT7, the only member of the 7 family in *Drosophila*, stimulates the production of cAMP [70,73]. Receptors of the 2 family, 5-HT2A and 5-HT2B in *Drosophila*, act through a the PLC-$IP_3$ signaling pathway to increase intracellular calcium [72,74,75]. Together, this diversity of receptors is thought to allow serotonin to produce complex physiological responses that depend on both synaptic connectivity and receptor expression patterns.

Before characterizing the phenotypes of these receptor mutants, we analyzed a mutant of the *Trh* gene ($Trh^{01}$), which is globally unable to produce serotonin [48]. Reassuringly, $Trh^{01}$ animals show a similar phenotype to animals in which 5-$HT^{VNC}$ neurons were silenced: the flies walk significantly faster and more frequently than controls, and exhibit a similar startle response in the earthquake paradigm (Figure 5A and B, Figure S5A,C-F). In addition, $Trh^{01}$ mutant animals walk closer to the edge of the arena compared to control animals, consistent with previous observations [46] (Figure S5A).

Null receptor mutants $5\text{-}HT1A^{Gal4}$, $1B^{Gal4}$, $2A^{Gal4}$, and $7^{Gal4}$ all increase the percentage of time animals spend walking (Figure S5A) [48]. However, an increase in walking speed is only observed in $5\text{-}HT7^{Gal4}$ mutants (Figure 5A and C), suggesting that 5-HT7 is the primary receptor responsible for mediating the effects of serotonin on walking speed.

We next tested the receptor mutants in the earthquake paradigm. Interestingly, $5\text{-}HT7^{Gal4}$ and $5\text{-}HT1B^{Gal4}$ mutants closely phenocopy the startle response seen in $Trh^{01}$ mutants and also in the 5-$HT^{VNC}$ inactivation experiments (Figure 5C and D, Figure S5E-H). By contrast, although $5\text{-}HT1A^{Gal4}$ and $5\text{-}HT2A^{Gal4}$ mutants speed up at the same rate as controls, they exhibit a sustained decrease in their final target speed in response to this stimulus (Figure 5E and F, Figure S5E, I, and J).

These data are consistent with the idea that different receptors influence distinct aspects of the startle response. Notably, mutation of receptors that are predicted to have opposing

effects on cAMP production, such as 5-HT1A and 5-HT7, can result in similar phenotypes. Further, some receptor mutants exhibit phenotypes that are not seen in *Trh*$^{01}$ mutant animals. These complex changes in locomotor behavior may be explained by the differential expression of serotonin receptors in key components of the locomotor circuit.

Figure 5

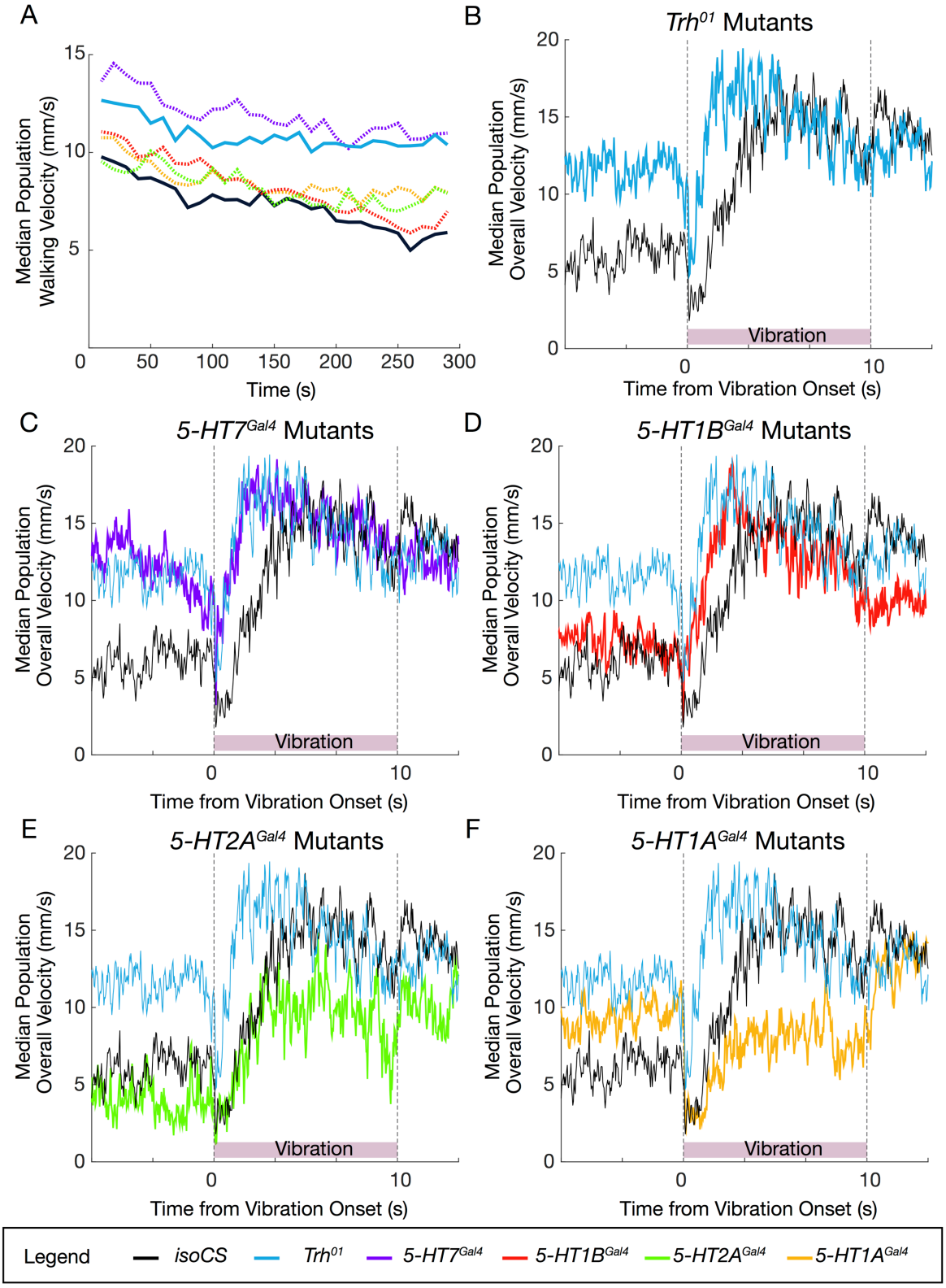


**Figure 5. Mutations in *Trh* and select serotonin receptors replicate 5-HT$^{VNC}$ inactivation**

**phenotype.**

**A.** Median population walking speed binned at ten second intervals for *Trh*$^{01}$ mutants (blue), which walk faster than background matched *isoCS* controls (black), consistent with the inactivation experiments. *5-HT7*$^{Gal4}$ mutants (purple) replicates this phenotype, but other mutants do not show a baseline increase in walking speed. N=130 *isoCS*, N=130 *5-HT1A*$^{Gal4}$, N=120 *5-HT1B*$^{Gal4}$, N=100 *5-HT2A*$^{Gal4}$, N=120 *5-HT7*$^{Gal4}$, N=120 *Trh*$^{01}$.

**B-F.** Median population walking speed sampled at 30 Hz in response to vibration stimulus. *Trh*$^{01}$ mutants (B, blue line) show a blunted and shortened pause in response to novel stimulus. *5-HT7*$^{Gal4}$ mutants (C, purple line) and *5-HT1B*$^{Gal4}$ mutants (D, red line) show a similar phenotype to *Trh*$^{01}$ mutants (blue line). *5-HT2A*$^{Gal4}$ mutants (E, green line) and *5-HT1A*$^{Gal4}$ mutants (F, yellow line) have a pause phase comparable to controls, but do not accelerate as much in response to the vibration stimulus.

## Serotonin receptors are expressed in distinct cell types

The different effects on walking observed in flies mutant for different serotonin receptors suggest that, in addition to distinct biochemical properties, they also have different expression patterns within the locomotor circuit. To identify neurons that express these receptors, we used gene and protein trap Gal4 lines from the MiMIC library to drive expression of a GFP reporter in the pattern of each receptor subtype [76] (Figure S6G). Each receptor line drove expression in many neurons both within the brain and the VNC (Figure 6A-E). Many of these are uncharacterized interneurons that cannot yet be functionally studied. However, each serotonin receptor is also expressed in distinct subsets of leg motor and sensory neurons. In particular, while members of the 5-HT1 family are predominantly expressed in mechanosensory neurons throughout the leg, 5-HT2 and 5-HT7 receptors are expressed in proximal-targeting flexor and extensor motor neurons (Figure S6A-F), proprioceptive, and distal sensory neuron populations (Figure 6F-K). Thus, serotonin release in the VNC is likely to differentially affect these components of the locomotor circuit, ultimately contributing to the observed changes in behavior.

Figure 6

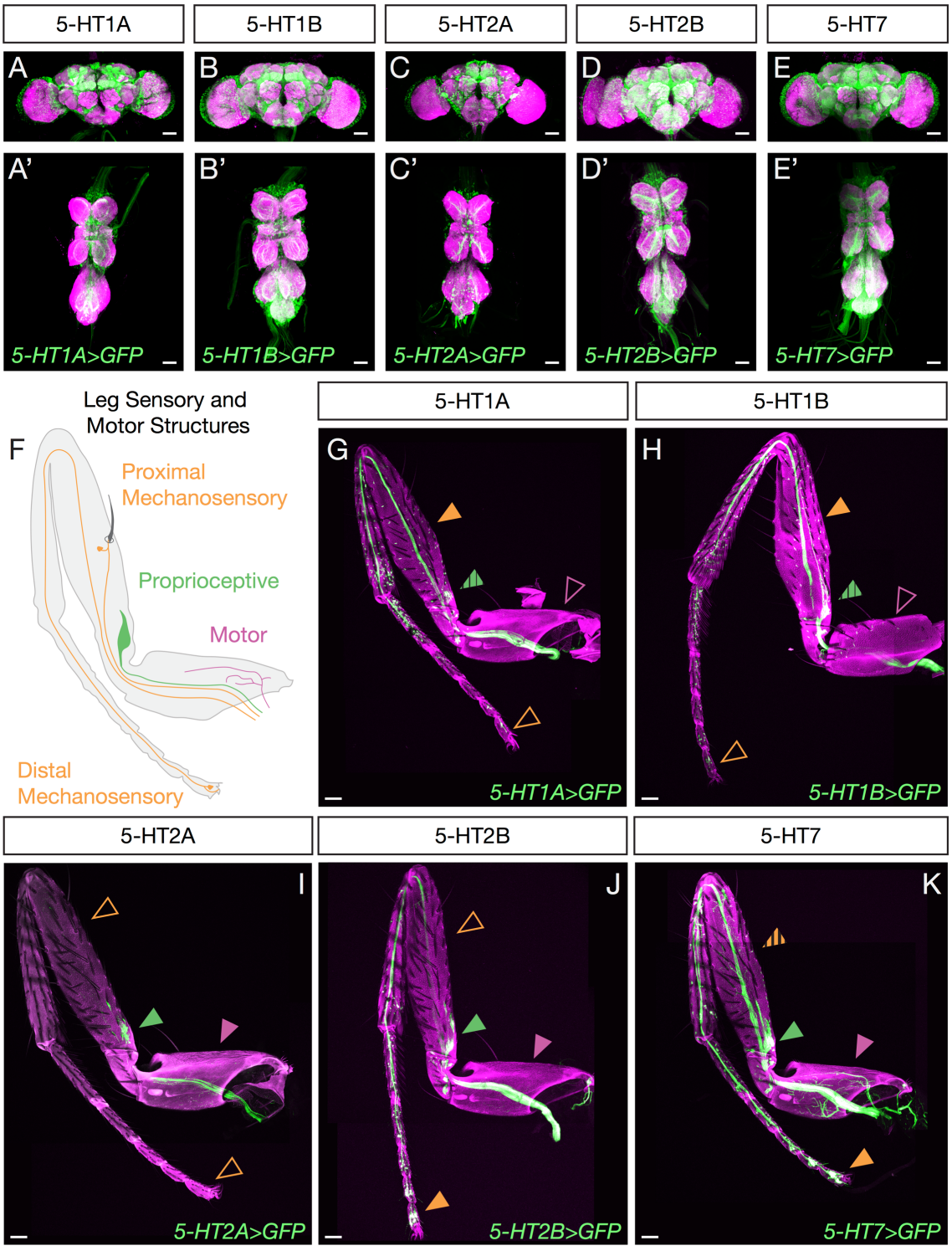


**Figure 6. Serotonin receptors are differentially expressed in locomotor circuitry components, including sensory and motor neurons.**

**A-E.** Maximum intensity projections show Gal4-driven expression of serotonin receptors in both the brain and VNC. All scale bars are 50 μm.

**F.** Schematic of sensory and motor neuron populations innervating the adult leg.

**G-K.** Maximum intensity projections show Gal4-driven expression of serotonin receptors in neuronal processes in the adult T1 leg. Each receptor is expressed in a distinct pattern in sensory-motor components. While some are expressed in motor neurons (purple arrows, hatched arrows indicate limited or weak expression) and proprioceptive neurons (green arrows), others are not. All receptors are expressed in a subset of mechanosensory neurons (orange arrows), but some are preferentially expressed in proximal or distal leg segments. All scale bars are 50 μm.

## Discussion

Walking is highly stereotyped, consisting of a small number of well-defined gaits, each with its own set of characteristic kinematic parameters. However, these highly stereotyped gaits must also be flexible, to adapt to a wide variety of environments, complex terrains, and novel situations. How nervous systems manage to orchestrate behaviors that are simultaneously stereotyped and flexible is not well understood. Here we show in the fly that (i) serotonergic VNC neural activity modulates walking speed in a context-independent manner and (ii) these neurons play a critical role in a fly's ability to modulate its walking behavior in response to the sudden onset of a startling stimulus. Moreover, the multiple roles the serotonergic system plays are mediated by distinct receptors, which have different biochemical properties and are expressed in unique subsets of locomotor circuit components.

### A common role for serotonin in modulating walking speed across species

A central finding of our study is that serotonergic neuron activity in the VNC modulates baseline walking speed. This finding strongly parallels previous observations in the motor systems of other organisms. For example, activity of serotonergic neurons in the cat brainstem is correlated with motor behavior and walking speed [12,77,78]. Additionally, in vertebrates as diverse as the lamprey and mouse, serotonin induces an increase in step cycle period, slowing locomotor rhythms (reviewed in [42]). One recent study in mice showed that activation of the dorsal raphe nucleus – a key serotonergic brain region – produces rapid suppression of spontaneous locomotion and locomotor speed, while showing minimal effect on kinematic parameters, such as gait, or on non-locomotor behaviors such as grooming [79]. These parallels to our results suggest that the modulatory role of the serotonergic system in regulating locomotor speed is remarkably conserved across the animal kingdom.

453
454 **Serotonergic modulation of the startle response**

455 In our experiments, we consistently observed that the onset of a startling stimulus (be it
456 visual or mechanosensory), induces a brief period of pausing behavior in wild type flies. We
457 hypothesize that these behavioral pauses are similar to startle responses seen in both
458 mammalian systems and insects, which also trigger a pause phase before animals embark on
459 an appropriate behavioral action [63,64,67,68,80-82]. While the importance of these pausing
460 behaviors remains poorly understood, it may be that they allow animals to collect additional
461 sensory information before they select an appropriate response to the startling stimulus.

462 We find that inactivation of the VNC serotonergic system does not completely abolish
463 this startle response, suggesting that this system is not the primary driver of this behavior, but
464 instead serves to modulate the latency of the response following an initial freeze phase when
465 animals stop. A role for serotonin in the startle response appears to be conserved: In mammals,
466 the absence of serotonin, due to the lesion of key serotonergic brain regions or pharmacological
467 blockade, is generally associated with an increase in the intensity of startle responses [83,84].
468 Although this may seem counter to our results, other studies have shown that serotonin
469 increases startle responses when injected directly into the lumbar spinal cord [85-88]. Thus,
470 serotonin may play distinct roles in the forebrain and in the spinal cord. Together with our
471 results, we suggest that the role of spinal cord/VNC serotonin release is to extend the latency
472 period and/or amplify the startle response.

473

474 **Serotonin acts differentially on sensory and motor circuitry to modulate walking**

475 Based on the distribution of receptors in locomotor circuitry components, we can
476 formulate a preliminary model of how serotonergic action may be working to modulate
477 *Drosophila* locomotor circuits both at the level of sensory input and motor output. We note,
478 however, that this model is likely incomplete as we cannot as of now incorporate the role that
479 local interneurons that also express 5-HT receptors play in modulating locomotion behavior.
480 Nevertheless, because the primary receptors expressed in motor neurons are 5-HT7 and 5-
481 HT2B, which have been shown to upregulate the production of cAMP and facilitate calcium
482 entry [72,89], we hypothesize that the phenotypes we observe are due at least in part to
483 serotonin action on these cells.

There is ample evidence in the literature to support this role for serotonin both in rodent models as well as in human studies (reviewed in [90-92]). While increased motor output is usually correlated with increased, not decreased, speed [93], increased muscle output has also been shown to be required in humans to navigate complex terrain, and may be playing a similar role in the fly [94,95]. In addition, it is noteworthy that the motor neurons expressing these receptors target both flexor and extensor muscles in the coxa and femur, two proximal leg segments (Figure S6A-F). These observations suggest that serotonin acting on these motor neurons may result in co-contraction, a mechanism that facilitates joint stability in the face of a complex environment and also during the preparatory phase for certain escape behaviors [66,94-99]

In addition to a potential role in motor neurons, serotonin receptors are expressed in distinct classes of leg sensory neurons that target the leg neuropils of the VNC. We hypothesize that this distribution of receptors serves to shift the balance of sensory information in response to serotonergic input. Based on the known downstream signaling properties of these receptors, we predict that increased levels of serotonin in the VNC would amplify proprioceptive and distal sensory inputs at the expense of more proximal sensory information. These shifts in sensory processing may also contribute to increased stability and might be useful in other contexts where slow walking is preferred, such as navigating complex terrains where improved sensory information might be beneficial.

Considering the broad expression of serotonergic receptors in sensory organs, it is interesting that one of the behavioral roles of serotonin we identified is its ability to mediate the response to vibration. Vibration is sensed by the chordotonal organ, and our expression analysis reveals that serotonin receptors are expressed to different extents in chordotonal neurons [100-102]. Together, these observations suggest that modulation of sensory information as it is entering the VNC plays a key role in how serotonin modulates the response to a vibration stimulus. In addition, the observation that serotonin release in the VNC affects the response to both the earthquake and blackout paradigms similarly, which are perceived by two very different sensory systems, suggests that this neuromodulator is controlling downstream locomotor components, such as motor neurons, that are shared by both systems.

## Experimental Procedures

### Fly husbandry:

Unless otherwise described, flies were maintained at 25° C on dextrose cornmeal food using standard laboratory techniques. Crosses used for behavioral experiments were flipped every 2-3 days to prevent overcrowding. For all arena experiments, flies were maintained on Nutrifly German Sick food (Genessee Scientific 66-115) in an incubator humidified at 60% with a 12h:12h light:dark cycle. As animals eclosed, females of the appropriate genotype were collected under $CO_2$ anesthesia every 2-3 days. For non-optogenetic experiments, flies were collected onto Nutrifly Food without any additive. For optogenetic experiments, flies were collected onto Nutrifly food supplemented with either .4 mM ATR or an equal concentration of solvent alone (DMSO for Flywalker experiments, 95% EtOH for arena experiments). Animals were aged in the dark (for optogenetic experiments) or on the same light:dark cycle for 2-3 more days at 25° C before being assayed.

**Fly Strains:**

| Line | Source | Reference |
|---|---|---|
| *+ ; + ; Trh Gal4* | BL 38389 | [55] |
| *+ ; + ; TH Gal4* | | [56] |
| *+ ; Tdc2 Gal4 ; +* | | [57] |
| *$w^{1118}$ ; Iliso ; IIIiso* | BL 5905 | [103] |
| *$w^{1118}$ ; Iliso ; Trh-Gal4* | This study | |
| *$w^{1118}$ ; Iliso ; TH-Gal4* | This study | |
| *$w^{1118}$ ; Tdc2 Gal4 ; IIIiso* | This study | |
| *$w^{1118}$ ; Iliso ; Trh iso Gal4* | This study – 10x outcrossed | |
| *+ ; UAS-mCD8::GFP; +* | BL | |
| *tub>gal80> ; tsh-LexA, LexAop-Flp ; +* | Marta Zlatic | Kristin Scott |
| *+ ; tsh-Gal80 ; +* | Julie Simpson | |
| *+ ; + ; UAS-csChrimson::mVenus* | BL 55136 | [104] |
| *+ ; + ; UAS-Kir2.1* | BL 6595 | [59] |
| *+ ; + ; 20XUAS-hexameric-GFP* | Steve Stowers | [105] |
| *+ ; UAS-OpGCamp6f ; UAS-tdTomato* | Pavan Ramdya | [60] |
| *IsoCS* | Yi Rao | [48] |
| *w+ ; 5-HT1A$^{Gal4}$ ; +* | | |
| *w+ ; 5-HT1B$^{Gal4}$ ; +* | | |
| *w+ ; + ; 5-HT2A$^{Gal4}$* | | |
| *w+ ; + ; 5-HT7$^{Gal4}$* | | |
| *w+ ; + ; Trh$^{01}$* | | |
| *5-HT1A-Gal4 (MI04464)* | Herman A. Dierick | [76] |
| *5-HT1B-Gal4 (MI05213)* | | |
| *5-HT2A-Gal4 (MI00459)* | | |
| *5-HT2A-Gal4 (MI03299)* | | |
| *5-HT2B-Gal4 (MI05208)* | | |
| *5-HT2B-Gal4 (MI06500)* | | |
| *5-HT2B-Gal4 (MI07403)* | | |
| *5-HT7-Gal4 (MI00215)* | | |

| | | |
|---|---|---|
| *Vglut>>LexAVP16, LexO-CD8GFP /FM7; Vglut>>LexAVP16, UASFlp, LexO-CD8GFP /CyO; LexO-CD8GFP, LexO-CD8GFP, Vglut>>LexAVP16 /TM2* | Myungin Baek | |
| *+ ; MHC::RFP ; +* | BL 38464 | |

531
532 **Genotypes with associated Figures**
533

| Experimental Line | Main Figure | Supplementary |
|---|---|---|
| *+ /+ ; tsh Gal80 / UAS mCD8 GFP ; Trh Gal4 / +* | 1B, B', B'' | |
| *tub>gal80> / + ; tsh LexA, lexAop Flp / + ; Trh Gal4 / UAS mCD8 GFP* | 1C, C', C'' | |
| *+ /+ ; tsh Gal80 / +; UAS mCD8 GFP, TH Gal4 / +* | 1D, D', D'' | |
| *tub>gal80> / + ; tsh LexA, lexAop Flp / + ; TH Gal4, UAS mCD8 GFP / +* | 1E, E', E'' | |
| *+ /+ ; tsh Gal80 / Tdc2 Gal4 ; UAS mCD8 GFP / +* | 1F, F', F'' | |
| *tub>gal80> / + ; tsh LexA, lexAop Flp / Tdc2 Gal4 ; UAS mCD8 GFP / +* | 1G, G', G'' | |
| *tub>gal80> / $w^{1118}$ ; tsh LexA, lexAop Flp / isoII ; UAS csChrimson::mVenus / isoIII* | 1H<br>2A, C | S2D, F |
| *tub>gal80> / $w^{1118}$ ; tsh LexA, lexAop Flp / isoII ; UAS csChrimson::mVenus / Trh Gal4* | 1H<br>3A-M | S3 B<br>S4 D |
| *tub>gal80> / $w^{1118}$ ; tsh LexA, lexAop Flp / isoII ; UAS csChrimson::mVenus / TH Gal4* | 1H | |
| *tub>gal80> / $w^{1118}$ ; tsh LexA, lexAop Flp / Tdc2 Gal4 ; UAS csChrimson::mVenus / isoIII* | 1H | |
| *tub>gal80> / $w^{1118}$ ; tsh LexA, lexAop Flp / isoII ; UAS csChrimson::mVenus / Trh iso Gal4* | 2A, C | S1<br>S2D, F, H, I |
| *tub>gal80> / $w^{1118}$ ; tsh LexA, lexAop Flp / isoII ; UAS Kir2.1::GFP / isoIII* | 2B and C<br>4A-C | S2E and G |
| *tub>gal80> / $w^{1118}$ ; tsh LexA, lexAop Flp / isoII ; UAS Kir2.1::GFP / Trh iso Gal4* | 2B and C<br>4A-C | S2E, G, H, I<br>S5D and F |

| | | |
|---|---|---|
| *tub>gal80>/+ ; tsh-LexA, lexAop-FLP/UAS-opGCaMP6f; Trh-Gal4/UAS-tdTomato* | 2D-F | S4B, C, E, F |
| *isoCS* | 5A-F | S5A,C, E |
| *W+ ; 5-HT1A$^{Gal4}$ ; +* | 5A, F | S5A,C,J |
| *W+ ; 5-HT1B$^{Gal4}$ ; +* | 5A, D | S5A,C,H |
| *W+ ; + ; 5-HT2A$^{Gal4}$* | 5A, E | S5A,C,I |
| *W+ ; + ; 5-HT7$^{Gal4}$* | 5A, C | S5A,C,G |
| *W+ ; + ; Trh$^{01}$* | 5A-F | S5A,C-J |
| *5-HT1A-Gal4 (MI04464) / + ; 20X-UAS hexameric GFP / +* | 6A,G | S6G |
| *5-HT1B-Gal4 (MI05213) / + ; 20X-UAS hexameric GFP / +* | 6B,H | S6G |
| *+/+ ; 5-HT2A-Gal4 (MI00459) / 20X-UAS hexameric GFP* | 6C,I | S6G |
| *+/+ ; 5-HT2B-Gal4 (MI05208) / 20X-UAS hexameric GFP* | 6D, J | S6G |
| *+/+ ; 5-HT7-Gal4 (MI0215) / 20X-UAS hexameric GFP* | 6E, K | S6G |
| *+/+ ; 5-HT2A-Gal4 (MI03299) / 20X-UAS hexameric GFP* | | S6G |
| *+/+ ; 5-HT2B-Gal4 (MI06500) / 20X-UAS hexameric GFP* | | S6G |
| *+/+ ; 5-HT2B-Gal4 (MI07403) / 20X-UAS hexameric GFP* | | S6G |
| *Vglut>>LexA, LexO-CD8GFP / +; Vglut>>LexA, UASFlp, LexO-CD8GFP / +; LexO-CD8GFP, LexO-CD8GFP, Vglut>>LexAVP16 / 5-HT2B-Gal4 (MI05208)* | | S6A |
| *Vglut>>LexA, LexO-CD8GFP / +; Vglut>>LexA, UASFlp, LexO-CD8GFP / +; LexO-CD8GFP, LexO-CD8GFP, Vglut>>LexAVP16 / 5-HT7-Gal4 (MI0215)* | | S6B |
| *Vglut>>LexA, LexO-CD8GFP / +; Vglut>>LexA, UASFlp, LexO-CD8GFP / MHC-RFP; LexO-CD8GFP, LexO-CD8GFP, Vglut>>LexAVP16 / 5-HT2B-Gal4 (MI05208)* | | S6C |
| *Vglut>>LexA, LexO-CD8GFP / +; Vglut>>LexA, UASFlp, LexO-CD8GFP / MHC-RFP; LexO-CD8GFP, LexO-CD8GFP, Vglut>>LexAVP16 / 5-HT7-Gal4 (MI0215)* | | S6D |

534

## Immunostaining brain and VNC

Brains and VNCs were dissected in phosphate buffered saline with 0.3% Triton (PBST) and fixed in 4% Paraformaldehyde (PFA) for 20 minutes. Samples were washed five times for 20 minutes in PBST with 0.1% Bovine serum albumin (BSA), and then blocked in PBST-BSA for one hour at room temperature, or overnight at 4° C. Samples were incubated with primary antibody diluted in PBST-BSA overnight at 4° C, and washed five times 20 minutes with PBST-BSA the next day. Samples were then incubated in secondary antibody diluted in PBST-BSA overnight at 4° C. The next day, samples were washed five times for 20 minutes in PBST, and then the liquid was replaced with Vectashield and samples were incubated overnight prior to mounting. Brains and VNCs from the same animals were mounted together, with the ventral surface of the VNC and the anterior surface of the brain facing up.

Validation of expression patterns during two photon experiments were performed as described in [60].

**Antibodies:**

| Antibody | Source | Concentration | Animal | Figure | SFig |
|---|---|---|---|---|---|
| Vglut | Aaron DiAntonio | 1:10,000 | rb | | S1J |
| 5-HT | Sigma | 1:1000 | rb | | S1E, S4D' |
| TH | Immunostar | 1:1000 | m | | S1F |
| ChAT | DHSB | 1:500 | m | | S1I |
| Brp-c | DHSB | 1:20 – 1:100 | m | 1B-G, 6A-E | S4B |
| GABA | Sigma | 1:1000 | rb | | S1H |
| Tdc2 | Cova Labs | 1:200 | rb | | S1G |
| dsRed | Takara Bio | 1:1000 | rb | | S4 B |

| Animal | Fluorophore | Concentration | Source |
|---|---|---|---|
| r | Alexa 488 | 1:500 | Invitrogen |
| rb | Alexa 555 | 1:500 | Invitrogen |
| m | Alexa 647 | 1:500 | Invitrogen |
| Goat anti rb | Cy3 | 1:400 | Jackson |
| Goat anti m | Alexa 633 | 1:400 | Thermofisher |

## Confocal Imaging

Mounted brains and VNCs were imaged on a Leica TCS SP5 confocal at 20X magnification with a resolution of 1024 x 512 pixels, and at a scanning rate of 200 Hz and 3x averaging. Sections were taken at 1 um increments. Laser power and detector gain were maintained constant for the brain and VNC of the same animals, but were adjusted for optimal signal between animals.

Imaging of fixed samples following two photon live imaging experiments was performed on a Zeiss LSM 700 Laser Scanning Confocal Microscope at 20X magnification and 2X averaging, with a 0.52 X 0.52 um pixel size. Z sections were taken at 1 um intervals. As described in [60].

## Cell Counting and Quantification

Images were analyzed in Fiji [106]. For quantification of the number of cells driven by *Trh-Gal4* in the brain and VNC, mVenus positive and 5-HT positive cell bodies were counted from five or more individual animals.

### Leg dissection, imaging, and image processing

To prepare legs for imaging, fly heads and abdomens were removed, and thoraces with legs attached were fixed overnight in 4% PFA at 4° C. Carcasses were washed 5 times with 0.03% PBST, and then place in Vectashield overnight before legs were mounted. Imaging was performed on a Leica SP5 confocal at 20X and 1024 x 1024 pixel resolution with 3x averaging, with sections taken at steps of 1 um. Two PMT detectors were set to capture green fluorescent signal and the green autofluorescence of the cuticle. Laser power was adjusted independently for each line to achieve optimal visualization of structures. Images were processed in Fiji [106]. Autofluorescence was subtracted from the green channel to allow for clearer visualization of leg structures.

## Behavioral Systems

## Arena Experiments

### Hardware

The skeleton of the system was built of 80-20 bars and acrylic plates and the arena itself was machined out of polycarbonate to the specifications published in [107]. The polycarbonate plastic arena was embedded in an aluminum plate to maintain a level surface. During experiments the arena was covered with an acrylic disc with a small hole for mouth pipetting in flies. The inside of the lid was coated in a thin layer of Fluon (Amazon, B00UJLH12A) to prevent flies from walking on the ceiling.

A Point Grey Blackfly Mono USB3 camera fitted with a Tamron 1/2" F/1.2 IR C-mount lens (B&H photo) was mounted above the arena and connected by USB 3 cable to a System 76 Leopard WS computer running Ubuntu 14.04 LTS. A Kodax 3x3" 89B Opaque IR filter (B&H photo) was placed in front of the camera detector to allow for detection of IR but not visible light.

Backlighting and optogenetic stimulation was provided by a plate of LEDs sitting under the arena. An acrylic diffuser was placed between the lighting plate and the arena. Each plate was designed with two sets of LEDs – one for IR backlighting (ledlightsworld.com SMD3528-300) and one for optogenetic or white light stimulation (superbrightLEDS.com NFLS-x-LC2 in Red or Natural White). These plates were swapped out when experiments required different color LEDs. To allow for detection of the on state of optogenetic lights, an additional IR light was wired in series with each visible light array, and placed within the field of view of the camera.

Each set of lights was powered separately by an Arduino Uno driver, allowing for modulation of light intensity via Pulse Width Modulation (PWM). Commands to set LED brightness and start and end experiments were sent to this driver using a PuTTY terminal and USB serial interface. For all the experiments described here, both IR and visible spectrum LEDs were set at 100% brightness. At the center of the arena this corresponded roughly to intensities of:

| Light On | Percent | Intensity | Wavelength Measured |
|---|---|---|---|
| Infrared | 100 | .13 mW | 1050 nm |

| | | | |
|---|---|---|---|
| | | .08 mW | 635 nm |
| | | .08 mW | 535 nm |
| Infrared + Red | 100 | .6 mW | 635 nm |
| Infrared + White | 100 | .62 mW | 635 nm |
| | | .68 mW | 535 nm |

**Data Acquisition**

All behavioral recordings were done during the three-hour morning activity peak. Prior to the experiment, the arena was leveled, the lid cleaned, and a new layer of Fluon applied. For each experiment, videos were recorded of cohorts of ten flies. For each recording session, flies were mouthpipetted into the arena through a small hole and then the arena lid was slid to move the hole out of the field of view. A blackout curtain cover (Thor Labs, BK5) was used to surround the arena, protecting it from any contaminating light.

Experimental protocols were programmed into the Arduino through serial communication via a PuTTY terminal. Videos were recorded at a rate of 30 frames per second and stored in a compressed "fly movie format" using custom software written by Andrew Straw at the University of Freiberg based on work previously described [108].

*Orientation experiments:* For inverted experiments, animals were introduced into the arena set-up when it was upright, and the lid of the arena was taped in place. The entire arena was manually inverted and propped up on two overturned ice buckets. Flies were either recorded upright and then inverted, for six minutes each, or in the opposite order. As no indicator was present to identify the moment of inversion, the first five minutes and the final five minutes of the video were selected as the before and after orientation switch periods.

*Starvation:* 24 hours prior to behavioral assay, half of the flies were transferred to an empty tube with a wet Kim Wipe. Behavioral recordings were collected as described above and lasted for five minutes.

*Heat:* Heated experiments were carried out inside a walk-in temperature-controlled incubator, which was set at either 18, 25, 30, or 37 C and 40% humidity. Flies were introduced to the arena immediately after entering the temperature-controlled room, recording began immediately thereafter and lasted for five minutes.

*Light:* For experiments examining responses to light stimuli, flies were first exposed to five minutes of white light, and then a one minute period of darkness.

*Vibration:* To provide a vibration stimulus, four 3V haptic motors (1670-1023-ND, Digikey) were attached to the aluminum plate in which the arena sat using 3D printed holders. The motors were wired in series and driven by the same Arduino system driving the arena's LED lighting array. For all experiments described, vibration was set at 10% power. The protocol for vibration experiments consisted of a brief habituation period (five minutes for inactivation experiments, 30 seconds for mutant experiments) followed by a 10 second vibration pulse and a 110 sec recovery period.

**Tracking**

Videos were tracked using the FlyTracker software from the Caltech vision lab [109]. Prior to tracking, pixel to mm conversion was calibrated using an inbuilt GUI. One calibration file was generated for all videos taken on the same day. Background model and thresholds were adjusted to provide optimal recognition of animals and were not standardized between recording sessions. If present, the state of an indicator light was annotated by custom-written MATLAB software.

**Behavioral classifiers**

*Jump*: Jumps were classified as frames where the velocity of the animal exceeded 50 mm/s.

*Walk*: Walking frames were defined using a dual threshold Schmitt trigger filter. Speed thresholds were set at 1 and 2.5 mm/s, and time thresholds were 0.1 s. Walking frames were also specified to be those in which the fly was not already engaged in a jump.

*Stop*: Stop frames were classified as any frames where animals were not performing walking or jumping behaviors.

**Parameters**

*Walk Frequency*: the percent of frames classified as walking during the recording period.

*Overall Velocity*: the median of all velocities over the recording period.

*Walking Velocity*: the median of velocities during all frames when the animal is classified as walking.

*Maximum Walking Velocity*: the maximum velocity an animal reaches during walking.

*Angular velocity*: the median value of angular velocity. This parameter takes into account directionality of turning.

*Absolute Angular Velocity*: the median of the absolute value of angular velocities. This parameter does not take into account directionality of turning.

*Distance from Wall*: the median distance from the closest point on the arena wall during the recording period.

*Walking bout number*: bouts were defined as contiguous frames of walking (longer than .1 s as specified in the walking classifier). The number of bouts was calculated for the entire recording period.

*Walking bout duration*: the length of each bout was calculated, and the median of all bout lengths was taken for each animal.

*Stop bout number and duration*: calculated as for walking bouts.

*Jump Frequency*: the percent of time that an animal spends in the jump state as defined above.

**Statistics**

For optogenetic arena experiments, behavior during the five-minutes before optogenetic lights were turned on was compared to behavior for five minutes of the light on period for each individual, with a 30 second buffer period after the light was turned on to avoid contamination from behavioral reaction to the light itself. For each activation experiment, we recorded behavior from both experimental (*Trh* ∩ *tsh* > *csChrimson*) and control ($w^{1118}$ ∩ *tsh* > *csChrimson*) flies. Prior to these experiments, the *Trh Gal4* line was outcrossed 10 times to our isogenized $w^{1118}$ control to ensure experimental and control backgrounds were genetically matched. For each genotype, we analyzed data from flies that had been fed with ATR, the required co-factor for optogenetic activation, and flies from the same cross that had been fed on food depleted of ATR. Figures show comparisons between ATR+ control and experimental animal behavior, as we found these populations had the most similar light off behavior pattern. However, significant differences in parameters are consistent even when all controls are included in the analysis.

For constitutive inhibition arena experiments, behavior during the five-minute light off period was analyzed for experimental (*Trh* ∩ *tsh* > *Kir2.1*) and control ($w^{1118}$ ∩ *tsh* > *Kir2.1*) flies fed on the same ATR negative food we used for optogenetic experiments. Prior to these experiments, the *Trh Gal4* line was outcrossed 10 times to our isogenized $w^{1118}$ control to ensure experimental and control backgrounds were genetically matched.

All analysis on data from arena experiments was performed in MATLAB using custom-written scripts. For normally distributed data, groups were compared by t-test. For non-normal data, groups were compared using Kruskal-Wallis analysis with Dunn-Sidak multiple correction testing when multiple groups were being compared. To compare changes in velocity distribution, bootstrapping was used to estimate the median difference between two genotypes and fit a 95% confidence interval around this difference.

The statistics performed associated with particular experiments is described in the figure legend for that experiment.

## Flywalker Experiments

### Hardware

The Flywalker was constructed as described in [10] with modifications. The rig consists of a frame of 80/20 supporting a sheet of 6 mm Borofloat optical glass with polished edges placed over an Andor Zyla 4.2 Magapixel sCMOS camera with an AF Nikkor 24-85mm 1:2.8-4 D lens (Nikon). On each edge of the glass were placed four Luxeon Neutral White (4100K) Rebel LED on a SinkPAD-II 10mm Square Base (230 lm @ 700mA) wired in series. Each set of lights was driven by a dedicated 700mA, Externally Dimmable, BuckPuck DC Driver (Luxeon), and all four of these drivers were connected to a single power supply. Each driver was independently adjustable.

Chambers were 3D printed by Protolabs. The ceiling of the chamber was painted with Fluon mixed with india ink, to prevent flies from walking on the ceiling. Small far-red LEDS were embedded in the walls of the chamber for Chrimson optogenetic experiments (LXM3-PD01 LUXEON). These lights were controlled by an Arduino driver that used pulsewitdth modulation to adjust light brightness. Commands were sent to this driver using a PuTTY terminal and USB serial interface. For all the experiments described here, LEDs were set at 20% brightness.

### Data Acquisition

The Flywalker was calibrated using a calibration reticle prior to use on each day. On the day of the experiment, 2-5 day old females were mouthpipetted into a clean glass tube and allowed to equilibrate for five minutes to get rid of as much dirt and food as possible to prevent contamination of the glass surface. 2-3 flies were added to the chamber by mouth pipette.

Videos were recorded using the NIS Elements AR software. A constant region of interest was defined such that the frame rate of recording was 226 fps. Each group of animals was recorded for one minute. Videos were cut to select traces where flies walked straight for >6 steps without other flies in the frame or touching the wall.

**Tracking**

Flywalker videos were automatically tracked using custom software written by Imre Bartos as described in [10]. Tracking was then validated by eye and incorrect footprint calls were corrected. Summary plots were then screened by eye for gross errors and for linear traces. If traces were short (<3 traces per foot) or excessively turning, they were excluded.

**Parameters**

Behavioral parameters were calculated as described in [10]. Gait parameters were defined as follows. Leg order in combination: LF RF LM RM LH RH. 1 indicates the leg is in stance phase, 0 indicates the leg is in swing phase.

| Tripod | Tetrapod | Wave | Non-Canonical |
|---|---|---|---|
| 100110 | 011011 | 011111 | All Other |
| 011001 | 011110 | 101111 | |
| | 100111 | 110111 | |
| | 110110 | 111011 | |
| | 101101 | 111101 | |
| | 111001 | 111110 | |

**Statistics**

For optogenetic Flywalker experiments, behavior was recorded for a one minute walking bout with red light illumination. Light off conditions were not possible as the white light LEDs required to generate fTIR signal contained the red wavelength used to activate our optogenetic tool. For each activation experiment, we recorded behavior from both experimental (*Trh – or other neuromodulatory Gal4 driver – ∩ tsh > csChrimson*) and control ($w^{1118}$ *∩ tsh > csChrimson*) flies. Neuromodulatory Gal4 driver lines had not been fully isogenized prior to these experiments, but two of three chromosomes (i.e., the chromosomes not containing the Gal4 itself) had been fully swapped out for those of our isogenized $w^{1118}$ control. For each genotype, we analyzed data from flies that had been fed with ATR, the required co-factor for optogenetic activation, and flies from the same cross that had been fed on food depleted of ATR. Figures show comparisons between ATR+ and ATR- controls, as we believe these populations provide the best genetic control and had the most similar behavioral pattern. However, significant differences in parameters are consistent even when all controls are included in our multivariate model (described below).

Statistical analysis of Flywalker data was performed using custom scripts written in MATLAB and R. For each walking bout, an average was calculated for every parameter across three to

five footprints per leg. For parameters that exponentially related to speed, the natural logarithm was taken of both the bout speed and parameter values. A multivariable regression model was then run on the data for every kinematic parameter. The formula for this model was as follows:

y ~ speed * ATR

This model was designed to analyze the effects of genotype and ATR while controlling for speed, which is the largest contributor to behavioral shifts.

We also ran a version of this model that contained all control data, to validate our results:

y ~ speed * Genotype * ATR

To prevent model overfitting, we selected our model based on Akaike information criterion using the R step() package.

## Functional Imaging Experiments

Functional imaging experiments on *Trh ∩ tsh > opGCaMP6f, tdTomato* animals were performed and analyzed as described in [60] with the following changes.

**Analysis protocol:**

*Initial image Processing:* TIFF videos from two-photon microscopy were processed in Fiji to merge green (opGCaMP6f) and red (tdTomato) channels [106]. No brightness or contrast adjustments were performed, in order to standardize region-of-interest (ROI) selection.

*ROI Selection:* The tdTomato channel was used to select ROIs containing neuronal processes, using custom Python software relying on OpenCV and Numpy libraries. Images were converted into 8-bits, color ranges were extended, and contrast was augmented to better detect ROIs. Baseline signals were subtracted and then brightness was scaled to a maximum value was 255. A blur filter was applied to the image (blur value =10), and then an Otsu Threshold was applied to binarize the grayscale image. After the image was thus thresholded, an erosion function (kernel size 5) was used to avoid the detection of overly large or small ROIs. The contours of all ROIs were detected on the eroded image and a copy of the contrast-augmented image was returned with ROI contours drawn super-imposed. A minimum threshold of 150 pixels was set on the ROI size to avoid overly small detections.

*Fluorescence extraction:* Mean fluorescence values for the tdTomato, or opGCaMP6f channels were calculated over all ROIs combined. Baseline signals for dF/F calculations were defined as mean raw fluorescence binned over 2.5 s.

*Synchronization:* Fluorescence measurements, behavior videography, and optic flow of spherical treadmill rotations were all recorded at different frame rates. Thus, we used interpolation to upsample fluorescence signals and behavioral videography acquisition rates to that of optic flow. Optic flow and fluorescence data were then smoothed (window size 200 ms). Optic flow data was then translated into mm/s in the anterior-posterior and medial-lateral directions and into degrees/s for yaw.

*Automatic Walking Classifier:* An automatic walking classifier was used to define walking bouts. A velocity of 0.31 mm/s was empirically determined as a threshold for distinguishing between walking and standing. The minimum threshold for bout length was empirically set to 2 s.

*Manual behavioral annotation:* Videos showing a side view of the fly on the spherical treadmill were manually annotated to capture four behaviors: (1) walk, (2) stop, (3) proboscis extension reflex, and (4) groom. All frames that could not neatly be classified as one of these four behaviors were defined as (5) other.

**Statistics**

*Manually Annotated Behaviors*: For each animal, the average dF/F for frames labeled a particular behavior classification was calculated. Comparisons between behaviors were made using Kruskal-Wallis testing with Dunn's correction for multiple comparisons.

*Timecourses*: For each behavioral classification, an average time course was determined for each animal by averaging dF/F for all behavioral bouts, centering them on bout onset. Averages across all animals were then calculated, and 95% confidence intervals fit by bootstrapping.

*Correlation Analysis*: To calculate the correlation between walking velocity and dF/F, we used a Pearson correlation to calculate R.

**Acknowledgements**

We thank Cesar Mendes for helping to optimize the Flywalker system, Imre Bartos for his help in updating the Flywalker analysis code, Andrew Straw for editing his motmot video collection software to make it compatible with our system, Meredith Peterson, Floris van Bruegel, Irene Kim and Michael Dickinson for assistance in building the arena hardware and data analysis approaches, Randy Bruno for assistance with analysis approaches, Laura Hermans in the Ramdya lab for her assistance with data analysis. We thank Daniel Wolpert for comments on the manuscript. This work was supported by NIH grants to R.S.M (1U01NS090514-01 and 1U19NS104655-01) the Columbia MD/PhD Training program (GM007367) and the Columbia Neuroscience Program (5T32NS064928-07). P.R. acknowledges support from the Swiss National Science Foundation (31003A_175667)

**Author contributions**

C.H. and R.S.M. conceived of the project and designed the experiments; T.T. and R.H. designed and built the behavior rigs; C.H. conducted all of the experiments and performed all data analysis, with the exception of calcium imaging experiments, which were carried out by C.-L.C. and analyzed by C.H., C.-L.C., and P.R.; C.H. and R.S.M. wrote the paper and P.R. edited it.

## References


[1] Ritzmann RE, Büschges A. Adaptive motor behavior in insects. Curr Opin Neurobiol 2007;17:629–36. doi:10.1016/j.conb.2008.01.001.

[2] Gibert P, Huey RB, Gilchrist GW. Locomotor performance of Drosophila melanogaster: interactions among developmental and adult temperatures, age, and geography. Evolution 2001;55:205–9.

[3] Blaesing B, Cruse H. Stick insect locomotion in a complex environment: climbing over large gaps. J Exp Biol 2004;207:1273–86.

[4] Ritzmann RE, Quinn RD, Fischer MS. Convergent evolution and locomotion through complex terrain by insects, vertebrates and robots. Arthropod Struct Dev 2004;33:361–79. doi:10.1016/j.asd.2004.05.001.

[5] Pick S, Strauss R. Goal-driven behavioral adaptations in gap-climbing Drosophila. Current Biology 2005;15:1473–8. doi:10.1016/j.cub.2005.07.022.

[6] Isakov A, Buchanan SM, Sullivan B, Ramachandran A, Chapman JKS, Lu ES, et al. Recovery of locomotion after injury in Drosophila depends on proprioception. J Exp Biol 2016. doi:10.1242/jeb.133652.

[7] Mendes CS, Rajendren SV, Bartos I, Márka S, Mann RS. Kinematic responses to changes in walking orientation and gravitational load in Drosophila melanogaster. PLoS ONE 2014;9:e109204. doi:10.1371/journal.pone.0109204.

[8] Wosnitza A, Bockemühl T, Dübbert M, Scholz H, Büschges A. Inter-leg coordination in the control of walking speed in Drosophila. J Exp Biol 2013;216:480–91. doi:10.1242/jeb.078139.

[9] Triphan T, Nern A, Roberts SF, Korff W, Naiman DQ, Strauss R. A screen for constituents of motor control and decision making in Drosophila reveals visual distance-estimation neurons. Sci Rep 2016;6:27000. doi:10.1038/srep27000.

[10] Mendes CS, Bartos I, Akay T, Márka S, Mann RS. Quantification of gait parameters in freely walking wild type and sensory deprived Drosophila melanogaster. Elifesciencesorg 2013. doi:10.7554/eLife.00231.

[11] Getting PA, Dekin MS. Mechanisms of pattern generation underlying swimming in Tritonia. IV. Gating of central pattern generator. J Neurophysiol 1985;53:466–80. doi:10.1152/jn.1985.53.2.466.

[12] Pearson KG. Common principles of motor control in vertebrates and invertebrates. Annu Rev Neurosci 1993;16:265–97. doi:10.1146/annurev.ne.16.030193.001405.

[13] Morton DW, Chiel HJ. Neural architectures for adaptive behavior. Trends Neurosci 1994;17:413–20.

[14] Harris-Warrick RM, Marder E. Modulation of neural networks for behavior. Annu Rev Neurosci 1991;14:39–57. doi:10.1146/annurev.ne.14.030191.000351.

[15] Graham D. Pattern and Control of Walking in Insects. In: Berridge MJ, Treherne JE, Wigglesworth VB, editors. Advances in Insect Physiology, vol. 18, Academic Press; 1985, pp. 31–140.

[16] Hughes GM. The Co-Ordination of Insect Movements. J Exp Biol 1952;29:267–85.

[17] Strauss R, Heisenberg M. Coordination of legs during straight walking and turning in Drosophila melanogaster. J Comp Physiol A 1990;167:403–12.

[18] Court RC, Armstrong JD, Borner J, Card G, Costa M, Dickinson M, et al. A Systematic Nomenclature for the Drosophila Ventral Nervous System. bioRxiv 2017. doi:10.1101/122952.

[19] Venkatasubramanian L, Mann RS. The development and assembly of the Drosophila adult ventral nerve cord. Curr Opin Neurobiol 2019;56:135–43.

doi:10.1016/j.conb.2019.01.013.

[20] Bässler U, Buschges A. Pattern generation for stick insect walking movements--multisensory control of a locomotor program. Brain Res Brain Res Rev 1998;27:65–88.

[21] Baek M, Mann RS. Lineage and birth date specify motor neuron targeting and dendritic architecture in adult Drosophila. J Neurosci 2009;29:6904–16. doi:10.1523/JNEUROSCI.1585-09.2009.

[22] Brierley DJ, Blanc E, Reddy OV, VijayRaghavan K, Williams DW. Dendritic targeting in the leg neuropil of Drosophila: the role of midline signalling molecules in generating a myotopic map. PLoS Biol 2009;7:e1000199. doi:10.1371/journal.pbio.1000199.

[23] Tuthill JC, Wilson RI. Mechanosensation and Adaptive Motor Control in Insects. Current Biology 2016;26:R1022–38. doi:10.1016/j.cub.2016.06.070.

[24] Murphey RK, Possidente DR, Vandervorst P, Ghysen A. Compartments and the topography of leg afferent projections in Drosophila. J Neurosci 1989;9:3209–17.

[25] Yellman C, Tao H, He B, Hirsh J. Conserved and sexually dimorphic behavioral responses to biogenic amines in decapitated Drosophila. Proc Natl Acad Sci USa 1997;94:4131–6.

[26] Graham D. Simulation of a Model for the Coordination of Leg Movement in Free Walking Insects 1977:1–12.

[27] Büschges A. Sensory control and organization of neural networks mediating coordination of multisegmental organs for locomotion. J Neurophysiol 2005;93:1127–35. doi:10.1152/jn.00615.2004.

[28] Pearson KG. Proprioceptive regulation of locomotion. Curr Opin Neurobiol 1995;5:786–91.

[29] Stein W, Büschges A, Bässler U. Intersegmental transfer of sensory signals in the stick insect leg muscle control system. J Neurobiol 2006;66:1253–69. doi:10.1002/neu.20285.

[30] Bekoff A, Nusbaum MP, Sabichi AL, Clifford M. Neural control of limb coordination. I. Comparison of hatching and walking motor output patterns in normal and deafferented chicks. J Neurosci 1987;7:2320–30.

[31] Grillner S, Zangger P. On the central generation of locomotion in the low spinal cat. Exp Brain Res 1979;34:241–61.

[32] Marder E, Bucher D. Central pattern generators and the control of rhythmic movements. Current Biology 2001;11:R986–96.

[33] Rossignol S, Dubuc R, Gossard J-P. Dynamic sensorimotor interactions in locomotion. Physiol Rev 2006;86:89–154. doi:10.1152/physrev.00028.2005.

[34] Weimann JM, Meyrand P, Marder E. Neurons that form multiple pattern generators: identification and multiple activity patterns of gastric/pyloric neurons in the crab stomatogastric system. J Neurophysiol 1991;65:111–22.

[35] Hooper SL, Marder E. Modulation of a central pattern generator by two neuropeptides, proctolin and FMRFamide. Brain Res 1984;305:186–91.

[36] Flamm RE, Harris-Warrick RM. Aminergic modulation in lobster stomatogastric ganglion. I. Effects on motor pattern and activity of neurons within the pyloric circuit. J Neurophysiol 1986;55:847–65. doi:10.1152/jn.1986.55.5.847.

[37] Flamm RE, Harris-Warrick RM. Aminergic modulation in lobster stomatogastric ganglion. II. Target neurons of dopamine, octopamine, and serotonin within the pyloric circuit. J Neurophysiol 1986;55:866–81. doi:10.1152/jn.1986.55.5.866.

[38] Hooper SL, Marder E. Modulation of the lobster pyloric rhythm by the peptide proctolin. J Neurosci 1987;7:2097–112.

[39] Nusbaum MP, Marder E. A neuronal role for a crustacean red pigment concentrating hormone-like peptide: neuroodulation of the pyloric rhythm in the crab, cancer

borealis. J Exp Biol 1988:165–81.

[40] Marder E. Neuromodulation of neuronal circuits: back to the future. Neuron 2012;76:1–11. doi:10.1016/j.neuron.2012.09.010.

[41] Barbeau H, Rossignol S. Initiation and modulation of the locomotor pattern in the adult chronic spinal cat by noradrenergic, serotonergic and dopaminergic drugs. Brain Res 1991;546:250–60.

[42] Harris-Warrick RM, Cohen AH. Serotonin modulates the central pattern generator for locomotion in the isolated lamprey spinal cord. J Exp Biol 1985;116:27–46.

[43] Parker D. Serotonergic modulation of locust motor neurons. J Neurophysiol 1995;73:923–32.

[44] Albin SD, Kaun KR, Knapp J-M, Chung P, Heberlein U, Simpson JH. A Subset of Serotonergic Neurons Evokes Hunger in Adult Drosophila. Curr Biol 2015;25:2435–40. doi:10.1016/j.cub.2015.08.005.

[45] Majeed ZR, Abdeljaber E, Soveland R, Cornwell K, Bankemper A, Koch F, et al. Modulatory Action by the Serotonergic System: Behavior and Neurophysiology in Drosophila melanogaster. Neural Plast 2016;2016:7291438. doi:10.1155/2016/7291438.

[46] Mohammad F, Aryal S, Ho J, Stewart JC, Norman NA, Tan TL, et al. Ancient Anxiety Pathways Influence Drosophila Defense Behaviors. Curr Biol 2016;26:981–6. doi:10.1016/j.cub.2016.02.031.

[47] Pooryasin A, Fiala A. Identified Serotonin-Releasing Neurons Induce Behavioral Quiescence and Suppress Mating in Drosophila. J Neurosci 2015;35:12792–812. doi:10.1523/JNEUROSCI.1638-15.2015.

[48] Qian Y, Cao Y, Deng B, Yang G, Li J, Xu R, et al. Sleep homeostasis regulated by 5HT2b receptor in a small subset of neurons in the dorsal fan-shaped body of drosophila. Elife 2017;6. doi:10.7554/eLife.26519.

[49] Pendleton RG, Rasheed A, Sardina T, Tully T, Hillman R. Effects of tyrosine hydroxylase mutants on locomotor activity in Drosophila: a study in functional genomics. Behav Genet 2002;32:89–94.

[50] Riemensperger T, Isabel G, Coulom H, Neuser K, Seugnet L, Kume K, et al. Behavioral consequences of dopamine deficiency in the Drosophila central nervous system. Proc Natl Acad Sci USa 2011;108:834–9. doi:10.1073/pnas.1010930108.

[51] Zhang W, Ge W, Wang Z. A toolbox for light control of Drosophila behaviors through Channelrhodopsin 2-mediated photoactivation of targeted neurons. Eur J Neurosci 2007;26:2405–16. doi:10.1111/j.1460-9568.2007.05862.x.

[52] Ueno T, Masuda N, Kume S, Kume K. Dopamine modulates the rest period length without perturbation of its power law distribution in Drosophila melanogaster. PLoS ONE 2012;7:e32007. doi:10.1371/journal.pone.0032007.

[53] Yang Z, Yu Y, Zhang V, Tian Y, Qi W, Wang L. Octopamine mediates starvation-induced hyperactivity in adult Drosophila. Proc Natl Acad Sci USa 2015;112:5219–24. doi:10.1073/pnas.1417838112.

[54] Brembs B, Christiansen F, Pflüger HJ, Duch C. Flight initiation and maintenance deficits in flies with genetically altered biogenic amine levels. J Neurosci 2007;27:11122–31. doi:10.1523/JNEUROSCI.2704-07.2007.

[55] Alekseyenko OV, Lee C, Kravitz EA. Targeted manipulation of serotonergic neurotransmission affects the escalation of aggression in adult male Drosophila melanogaster. PLoS ONE 2010;5:e10806. doi:10.1371/journal.pone.0010806.

[56] Friggi-Grelin F, Coulom H, Meller M, Gomez D, Hirsh J, Birman S. Targeted gene expression in Drosophila dopaminergic cells using regulatory sequences from tyrosine hydroxylase. J Neurobiol 2003;54:618–27. doi:10.1002/neu.10185.

[57] Cole SH, Carney GE, McClung CA, Willard SS, Taylor BJ, Hirsh J. Two functional but

noncomplementing Drosophila tyrosine decarboxylase genes: distinct roles for neural tyramine and octopamine in female fertility. J Biol Chem 2005;280:14948–55. doi:10.1074/jbc.M414197200.

[58] Riemensperger T, Issa A-R, Pech U, Coulom H, Nguyễn M-V, Cassar M, et al. A single dopamine pathway underlies progressive locomotor deficits in a Drosophila model of Parkinson disease. Cell Rep 2013;5:952–60. doi:10.1016/j.celrep.2013.10.032.

[59] Baines RA, Uhler JP, Thompson A, Sweeney ST, Bate M. Altered electrical properties in Drosophila neurons developing without synaptic transmission. J Neurosci 2001;21:1523–31.

[60] Chen C-L, Hermans L, Viswanathan MC, Fortun D, Aymanns F, Unser M, et al. Imaging neural activity in the ventral nerve cord of behaving adult Drosophila. Nature Communications 2018;9:459. doi:10.1126/science.1093173.

[61] Lee G, Park JH. Hemolymph sugar homeostasis and starvation-induced hyperactivity affected by genetic manipulations of the adipokinetic hormone-encoding gene in Drosophila melanogaster. Genetics 2004;167:311–23.

[62] Cho W, Heberlein U, Wolf FW. Habituation of an odorant-induced startle response in Drosophila. Genes Brain Behav 2004;3:127–37. doi:10.1111/j.1601-183x.2004.00061.x.

[63] Yeomans JS, Li L, Scott BW, Frankland PW. Tactile, acoustic and vestibular systems sum to elicit the startle reflex. Neurosci Biobehav Rev 2002;26:1–11.

[64] Yeomans JS, Frankland PW. The acoustic startle reflex: neurons and connections. Brain Res Brain Res Rev 1995;21:301–14.

[65] Bullock TH. Comparative Neuroethology of Startle, Rapid Escape, and Giant Fiber-Mediated Responses. In: Eaton RC, editor. Neural Mechanisms of Startle Behavior, Boston, MA: Springer US; 1984, pp. 1–13.

[66] Card GM. Escape behaviors in insects. Curr Opin Neurobiol 2012;22:180–6. doi:10.1016/j.conb.2011.12.009.

[67] Zacarias R, Namiki S, Card GM, Vasconcelos ML, Moita MA. Speed dependent descending control of freezing behavior in Drosophila melanogaster. Nature Communications 2018;9:3697. doi:10.1038/s41467-018-05875-1.

[68] Davis M. The Mammalian Startle Response. In: Eaton RC, editor. Neural Mechanisms of Startle Behavior, Boston, MA: Springer US; 1984, pp. 287–351. doi:10.1007/978-1-4899-2286-1_10.

[69] Saudou F, Hen R. 5-Hydroxytryptamine receptor subtypes in vertebrates and invertebrates. Neurochem Int 1994;25:503–32.

[70] Saudou F, Boschert U, Amlaiky N, Plassat JL, Hen R. A family of Drosophila serotonin receptors with distinct intracellular signalling properties and expression patterns. Embo J 1992;11:7–17.

[71] Hen R. Structural and functional conservation of serotonin receptors throughout evolution. Exs 1993;63:266–78.

[72] Tierney AJ. Invertebrate serotonin receptors: a molecular perspective on classification and pharmacology. J Exp Biol 2018;221:jeb184838. doi:10.1038/nature04216.

[73] Witz P, Amlaiky N, Plassat JL, Maroteaux L, Borrelli E, Hen R. Cloning and characterization of a Drosophila serotonin receptor that activates adenylate cyclase. Proc Natl Acad Sci USa 1990;87:8940–4.

[74] Blenau W, Daniel S, Balfanz S, Thamm M, Baumann A. Dm5-HT2B: Pharmacological Characterization of the Fifth Serotonin Receptor Subtype of Drosophila melanogaster. Front Syst Neurosci 2017;11:28. doi:10.3389/fnsys.2017.00028.

[75] Colas JF, Launay JM, Kellermann O, Rosay P, Maroteaux L. Drosophila 5-HT2 serotonin receptor: coexpression with fushi-tarazu during segmentation. Proc Natl

Acad Sci USa 1995;92:5441–5.

[76] Gnerer JP, Venken KJT, Dierick HA. Gene-specific cell labeling using MiMIC transposons. Nucleic Acids Res 2015;43:e56. doi:10.1093/nar/gkv113.

[77] Veasey SC, Fornal CA, Metzler CW, Jacobs BL. Response of serotonergic caudal raphe neurons in relation to specific motor activities in freely moving cats. J Neurosci 1995;15:5346–59.

[78] Veasey SC, Fornal CA, Metzler CW, Jacobs BL. Single-unit responses of serotonergic dorsal raphe neurons to specific motor challenges in freely moving cats. Neuroscience 1997;79:161–9.

[79] Correia PA, Lottem E, Banerjee D, Machado AS, Carey MR, Mainen ZF. Transient inhibition and long-term facilitation of locomotion by phasic optogenetic activation of serotonin neurons. Elife 2017;6. doi:10.7554/eLife.20975.

[80] Yilmaz M, Meister M. Rapid innate defensive responses of mice to looming visual stimuli. Curr Biol 2013;23:2011–5. doi:10.1016/j.cub.2013.08.015.

[81] Gibson WT, Gonzalez CR, Fernandez C, Ramasamy L, Tabachnik T, Du RR, et al. Behavioral responses to a repetitive visual threat stimulus express a persistent state of defensive arousal in Drosophila. Curr Biol 2015;25:1401–15. doi:10.1016/j.cub.2015.03.058.

[82] Card G, Dickinson MH. Visually mediated motor planning in the escape response of Drosophila. Current Biology 2008;18:1300–7. doi:10.1016/j.cub.2008.07.094.

[83] Davis M, Sheard MH. Habituation and sensitization of the rat startle response: effects of raphe lesions. Physiol Behav 1974;12:425–31. doi:10.1016/0031-9384(74)90120-6.

[84] Carlton PL, Advokat C. Attenuated habituation due to parachlorophenylalanine. Pharmacol Biochem Behav 1973;1:657–63. doi:10.1016/0091-3057(73)90029-4.

[85] Davis M, Strachan DI, Kass E. Excitatory and inhibitory effects of serotonin on sensorimotor reactivity measured with acoustic startle. Science 1980;209:521–3. doi:10.1126/science.7394520.

[86] Astrachan DI, Davis M. Spinal modulation of the acoustic startle response: the role of norepinephrine, serotonin and dopamine. Brain Res 1981;206:223–8. doi:10.1016/0006-8993(81)90121-9.

[87] Commissaris RL, Davis M. Opposite effects of N,N-dimethyltryptamine (DMT) and 5-methoxy-n,n-dimethyltryptamine (5-MeODMT) on acoustic startle: spinal vs brain sites of action. Neurosci Biobehav Rev 1982;6:515–20.

[88] Davis M, Astrachan DI, Gendelman PM, Gendelman DS. 5-Methoxy-N,N-dimethyltryptamine: spinal cord and brainstem mediation of excitatory effects on acoustic startle. Psychopharmacology (Berl) 1980;70:123–30. doi:10.1007/bf00435302.

[89] Tierney AJ. Structure and function of invertebrate 5-HT receptors: a review. Comp Biochem Physiol, Part a Mol Integr Physiol 2001;128:791–804.

[90] Perrier J-F, Cotel F. Serotonergic modulation of spinal motor control. Curr Opin Neurobiol 2014;33C:1–7. doi:10.1016/j.conb.2014.12.008.

[91] Perrier J-F, Rasmussen HB, Christensen RK, Petersen AV. Modulation of the intrinsic properties of motoneurons by serotonin. Curr Pharm Des 2013;19:4371–84.

[92] Johnson MD, Heckman CJ. Gain control mechanisms in spinal motoneurons. Front Neural Circuits 2014;8:81. doi:10.3389/fncir.2014.00081.

[93] Trinler U, Leboeuf F, Hollands K, Jones R, Baker R. Estimation of muscle activation during different walking speeds with two mathematical approaches compared to surface EMG. Gait & Posture 2018;64:266–73. doi:10.1016/j.gaitpost.2018.06.115.

[94] Voloshina AS, Kuo AD, Daley MA, Ferris DP. Biomechanics and energetics of walking on uneven terrain. J Exp Biol 2013;216:3963–70. doi:10.1242/jeb.081711.

[95] Cappellini G, Ivanenko YP, Dominici N, Poppele RE, Lacquaniti F. Motor patterns

during walking on a slippery walkway. J Neurophysiol 2010;103:746–60. doi:10.1152/jn.00499.2009.

[96] Wade C, Redfern MS, Andres RO, Breloff SP. Joint kinetics and muscle activity while walking on ballast. Hum Factors 2010;52:560–73. doi:10.1177/0018720810381996.

[97] Nakazawa K, Kawashima N, Akai M, Yano H. On the reflex coactivation of ankle flexor and extensor muscles induced by a sudden drop of support surface during walking in humans. J Appl Physiol 2004;96:604–11. doi:10.1152/japplphysiol.00670.2003.

[98] Heitler WJ, Burrows M. The locust jump. I. The motor programme. J Exp Biol 1977;66:203–19.

[99] Pearson KG, O'Shea M. Escape Behavior of the Locust. In: Eaton RC, editor. Neural Mechanisms of Startle Behavior, Boston, MA: Springer US; 1984, pp. 163–78.

[100] Field L, Matheson T. Chordotonal Organs of Insects. Advances in Insect Physiology 1998;27.

[101] Kavlie RG, Albert JT. Chordotonal organs. Curr Biol 2013;23:R334–5. doi:10.1016/j.cub.2013.03.048.

[102] Mamiya A, Gurung P, Tuthill JC. Neural Coding of Leg Proprioception in Drosophila. Neuron 2018;100:636–6. doi:10.1016/j.neuron.2018.09.009.

[103] Ryder E, Blows F, Ashburner M, Bautista-Llacer R, Coulson D, Drummond J, et al. The DrosDel collection: a set of P-element insertions for generating custom chromosomal aberrations in Drosophila melanogaster. Genetics 2004;167:797–813. doi:10.1534/genetics.104.026658.

[104] Klapoetke NC, Murata Y, Kim SS, Pulver SR, Birdsey-Benson A, Cho YK, et al. Independent optical excitation of distinct neural populations. Nat Methods 2014;11:338–46. doi:10.1038/nmeth.2836.

[105] Shearin HK, Dvarishkis AR, Kozeluh CD, Stowers RS. Expansion of the gateway multisite recombination cloning toolkit. PLoS ONE 2013;8:e77724. doi:10.1371/journal.pone.0077724.

[106] Schindelin J, Arganda-Carreras I, Frise E, Kaynig V, Longair M, Pietzsch T, et al. Fiji: an open-source platform for biological-image analysis. Nat Methods 2012;9:676–82. doi:10.1002/0471142727.mb1420s92.

[107] Simon JC, Dickinson MH. A new chamber for studying the behavior of Drosophila. PLoS ONE 2010;5:e8793. doi:10.1371/journal.pone.0008793.

[108] Straw AD, Dickinson MH. Motmot, an open-source toolkit for realtime video acquisition and analysis. Source Code Biol Med 2009;4:5. doi:10.1186/1751-0473-4-5.

[109] Eyjolfsdottir E, Branson S, Burgos-Artizzu XP, Hoopfer ED, Schor J, Anderson DJ, et al. Detecting Social Actions of Fruit Flies. In: Fleet D, Pajdla T, Schiele B, Tuytelaars T, editors. Cham: Springer International Publishing; 2014, pp. 772–87.